

## GRAIN BOUNDARIES: PHASE TRANSITIONS AND CRITICAL PHENOMENA

E. I. RABKIN, L. S. SHVINDLERMAN and B. B. STRAUMAL\*<sup>†</sup>

*Institute for Solid State Physics, Chernogolovka, Moscow distr., 142432 USSR*

*\*MPI für Metallforschung, Seestraße 75, 7000 Stuttgart 1, Germany*

Received 21 March 1991

Recent theories of grain boundary structure have been reviewed briefly. The possibility of existence of the same variety of phase transitions on grain boundaries as that on the crystal external surface has been demonstrated. Recent experimental data and theoretical models concerning grain boundary phase transitions are critically analysed. Grain boundary phase transitions connected with the formation of thin disordered layers on the boundary (prewetting, premelting) are particularly distinguished. Results of recent indirect experiments, which may be treated in terms of prewetting and premelting, have been reviewed. Experimentally observed critical phenomena in the vicinity of the prewetting transition on the tin-germanium interphase boundary have been discussed in terms of the critical exponents theory. Some ideas regarding directions of further research are presented.

### 1. Introduction

A grain boundary (GB) is a conjugation surface of two misoriented crystals. As well as a free surface of a crystal, the GB is a plane defect disturbing the translational symmetry of a crystal. The GBs are one of the most important defects in a solid; in many cases they define the mechanic, electric and magnetic properties of a polycrystal. However, the number of physical works devoted to GBs<sup>1</sup> is definitely less than that of external surface physics. There are some reasons for such a situation.

Firstly, the free surface plays the most important role in all emitting devices used in electronics and in the processes of adsorption and catalysis.

Secondly, the free surface is more “open” for investigation than GBs which are hidden inside a material. The progress achieved in the determination of a surface layer structure has been due to employment of such methods as low energy electron diffraction (LEED), scanning tunnel microscopy (STM), etc., which are not suitable for direct investigation of GBs.

Thirdly, interpretation of experimental results obtained in external surface investigations is simpler than in the case of GBs. Thus the distortion of a crystalline lattice structure near a surface may be characterized by one or two parameters (e.g. by change of a lattice period or interplanar spacing) while the

<sup>†</sup>Permanent address: Institute for Solid State Physics, Chernogolovka, Moscow 142432, USSR.

distortions even in the vicinity of the special boundaries of good matching (see below) are of a more complicated character.

Fourthly, for the performance of physically reproducible investigations on the GBs one must be able to reproduce the object of investigation itself. This is a difficult problem if the fact is taken into account that the position of a boundary in a crystal is defined by five geometric parameters. Moreover, the chemical composition of a material is of great importance. Materials of high purity are needed for the study of GBs just as for investigation of pure surface properties high vacuum is required.

It is obvious that all the above mentioned reasons are not of a principal character and do not justify the small attention given to the GBs as compared with that to the surface. Therefore, when writing this review we had in mind to show the possibility of existence of the same variety of phenomena (if not greater) on the GBs as that on the crystal external surface, and to draw the attention of physicists to this subject.

## 2. A Brief Review of the Grain Boundary Structure

The formal geometric theory ("crystallography") of the GBs<sup>2</sup> does not answer the question on the detailed structure of the boundary. The coordinates of individual atoms are determined by a specific form of interaction potentials, the contribution of thermal vibrations, the energy of electronic gas and other factors beyond the scope of a purely geometric theory. Such a theory is useful for estimation of the general properties of the boundary and is conditioned only by the fact that the two periodic crystalline lattices are conjugated over the boundary.

The most important notion of the geometric theory is the coincident sites lattice (CSL). The CSL defines the basic periodicity of the atomic structure of the GB. This lattice may be constructed by a shift of two misoriented lattices  $L1$  and  $L2$ , combining some parts of their two sites. All the coincident sites of two lattices after such a shift form CSL. Qualitatively, the CSL is characterized by the  $\Sigma$  value, which is the inverse density of coincident sites. It appears that the GB has a periodicity coinciding with that of the corresponding plane of the CSL. This periodicity is conserved even when the individual relaxation of atoms is taken into account.<sup>3</sup>

The other important notion of the theory is the lattice of pattern-conserving displacements (DSC). The vectors of this lattice determine a set of shifts of the  $L1$  lattice with respect to the  $L2$  one. This set retains the pattern of superposition of these lattices.

Near the some coincidence misorientations (as a rule with a low  $\Sigma$ ) GBs may have special properties: rather low energy, extremal mobility, diffusional permeability, etc. If the misorientation of crystallites somewhat differs from the coincidence one, the boundary may conserve a low-energetic structure due to GB dislocations (GBD) (in much the same way as it is achieved by steps on the

crystal surface). The value of deviation,  $\Delta\phi = \phi - \phi_c$  ( $\phi_c$  is the angle corresponding to the coincidence misorientation), is connected with the density of the GBDs  $n$ :

$$|\Delta\phi| = bn ,$$

where  $b$  is the Burgers vector value of the GBD. The  $b$  value is determined by the unit vectors of the DSC-lattice. Indeed if a cut is made along the boundary and one crystal is shifted with respect to the other by the vector of the DSC-lattice, then the boundary structure on both sides of the dislocation formed will be unchanged. This means that Burgers vector is indeed a vector of the DSC-lattice. It follows from the simple geometric theory that for a tilt boundary in a cubic lattice,

$$b = b_1 / \sqrt{\Sigma} ,$$

where  $b_1$  is the Burgers vector of a lattice dislocation. In order to distinguish between such GB dislocations and the lattice ones which are trapped to the boundary they should be called secondary GB dislocations (SGBD). The SGBDs in the boundaries of near-coincidence misorientations were observed in quite a number of works (whose review may be found in Ref. 3). The spacing between SGBDs, in the case of tilt boundaries, or the period of the screw SGBD grid in the case of a twist boundary are provided by the equation

$$d = b/2 \sin(\Delta\phi/2) .$$

The value of  $d$  must not be too small so that the cores of SGBD are not overlapped.

What boundaries should be called special? Or, this question may be formulated like this: is it possible to determine, knowing the five geometric parameters, that the boundary possesses extremal properties? In the 50s the question was not so doubtful: those boundaries were considered to be low energetic corresponding to either small  $\Sigma$  or high densities of coinciding sites on the boundary plane. However, it became obvious later that this was not always the case. By now the five various geometric criteria of low energetic boundaries have been proposed,<sup>4</sup> but none of them has been completely proven experimentally.

Nevertheless, the existence of special boundaries possessing low energies and extremal properties is experimentally confirmed. This fact, as well as the data of computer simulations of the structure of boundaries in Al and Cu<sup>5</sup> served as a base for structural units model. According to this model the structure of any boundary may be assumed as a mixture of two structural elements. These structural units are the "bricks" which compose the so-called delimiting boundaries nearest to the given one. The delimiting boundaries which are

preferable boundaries consist of one type of elementary structural units. They are, as a rule, special boundaries with low energy. The structure of any boundary is unambiguously determined: those structural units which are less in number must be placed as far from each other as possible. For instance, in the case of the symmetric tilt boundaries [100] in Cu the  $\Sigma 1$  (100),  $\Sigma 5$  (310),  $\Sigma 5$  (210), and  $\Sigma 1$  (110) boundaries are preferable.

The description of a boundary structure close to the coincidence one in terms of the structural units model permits one to complete a purely dislocation description. Let us consider delimiting boundaries composed from the structural units *A*. At a small change of a misorientation angle there will appear some structural units from the other delimiting boundary *B*. It turns out<sup>6</sup> that all the "additional" misorientation is gathered at the elements *B*, which therefore may be considered as the cores of SGBD. The Burgers vector of these dislocations must be determined in the DSC-lattice, corresponding to the boundary composed from the *A* units. It follows from this approach that the "gaps" corresponding to special boundaries on the dependences "property – misorientation angle" must be asymmetric.

As was mentioned above a dependence of any property of a GB on the misorientation angle of crystallites must have a non-monotonic character: at angles corresponding to the special boundaries, the extrema are to be observed on this dependence. However the situation may not be so simple. Figure 1 presents the misorientation dependences of the activation energy of migration, *E*, of the tilt boundaries [100] in bicrystals of Al on the different content of soluble impurities. One can see that in the purest samples this dependence is monotonic. At the impurity content of 0.0008 at% the minima corresponding to the special misorientations of 22.6, 28.1 and 36.9° are observed on this dependence, but at higher impurities contents the dependence becomes monotonic again.<sup>7</sup> The example presented shows clearly that a small amount of a soluble impurity can drastically change the properties of the GB.

### 3. Possible Types of GB Phase Transitions. Grain Boundary Melting

Since the GB symmetry is significantly lower than that of the crystal, phase transitions on the GBs accompanied by the formation of disordered interlayers near the boundary are likely to occur. GB melting is the most interesting phenomenon among such transitions. Quite a number of investigations have been undertaken to find it experimentally. The most direct way to reveal it is the study of wetting of a GB by the melt. In this case the boundary melting is accompanied by the angle  $\theta$  going to zero, where  $\theta$  is the dihedral angle at the vertex of a GB groove, formed at the site of contact of a solid metal with its liquid. This method was realized in Ref. 8. Bismuth films were observed in the column of the electron microscope under the condition that they were melting under the electron beam. Thus, the site of contact of a solid sample containing a boundary with its own

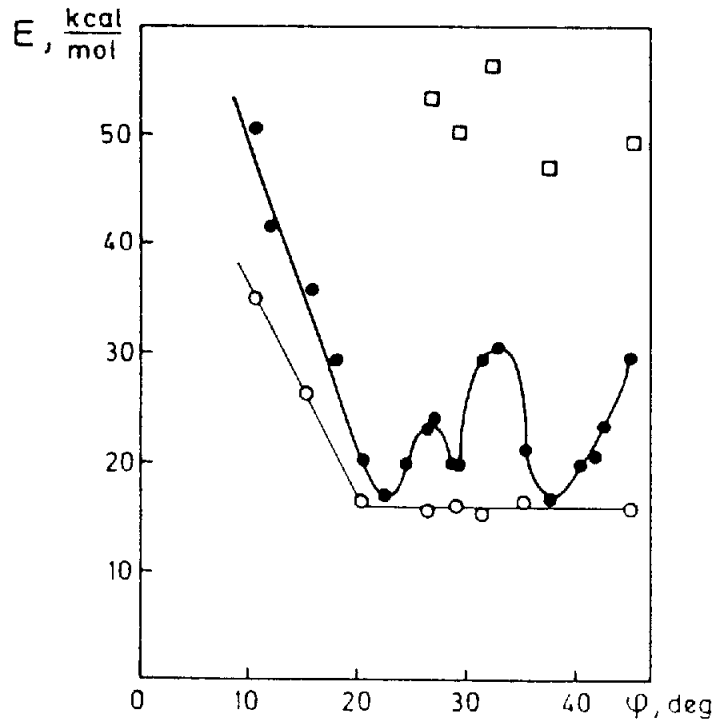


Fig. 1. The dependence of the activation energy of migration  $E$  for tilt grain boundaries [100] on the misorientation angle  $\phi$  in Al bicrystals of different purity<sup>7</sup>:  $\square$  — 99.98 at.% Al,  $\bullet$  — 99.9992 at.% Al,  $\circ$  — 99.99995 at.% Al.

melt have been studied *in situ*. It appeared that the dihedral angle  $\theta$  was decreasing as long as the misorientation angle  $\phi$  of grains was increasing, and at  $\phi^* \cong 7.5^\circ$  it abruptly fell from  $\theta^* = 34^\circ$  down to zero. Such behaviour of  $\theta$  may be connected with the peculiarities on the surface tension  $\sigma_{s1}$  “crystal-melt” dependence upon orientation. Rottman demonstrated, however, that the values  $\phi^*$  and  $\theta^*$  obtained in the experiment are not consistent with the symmetry conditions. Therefore it is most likely that thermodynamic equilibrium is absent in the measurements.<sup>9</sup>

Recently Hsieh and Balluffi tried to reveal GB melting<sup>10</sup> again. In bicrystals of Al containing the tilt boundaries [100]  $\Sigma 13$  ( $510$ ),  $\Sigma 17$  ( $410$ ),  $\Sigma 1$  ( $45^\circ$ ) and the twist boundary [100]  $\Sigma 1$  ( $45^\circ$ ), delocalization of the SGBD cores up to  $T = 0.96 T_{\text{melt}}$  was not observed. Moreover, the aluminum foil was heated in the microscope column so that this portion was melted. Upon this the expected amounts of a liquid phase were observed at a distance of  $15 \mu\text{m}$  from the boundary “foil-melt”. Estimates with the aid of thermal conductivity equation demonstrated the fact that on this portion of the foil the temperature differs from the melting temperature by not more than  $1^\circ$ . Based on this the authors<sup>10</sup> concluded that the GBs in aluminum do not melt up to  $0.999 T_{\text{melt}}$  although the boundaries are being wet by their own melt at  $T \cong T_{\text{melt}}$ .

In quite a number of works the question of high temperature behaviour of GBs was investigated by computer simulation techniques. Among them the most interesting are those where the molecular dynamics method (MD) was employed.

In the MD computations the trajectory of each atom composing the investigated sample is simulated by means of an immediate solution of the Newton motion equations. Thus the MD method (as distinguished from the Monte-Carlo method) yields a true picture of the dynamic behaviour of the system.

The results of all investigations performed on the large-angle boundary  $\Sigma 5$  show that, approaching the temperature of a crystal melting, the degree of disorder contributed by thermal vibrations grows faster in the boundary region than in the bulk. For the quantitative characteristic of thermal disorder the order parameter is usually employed<sup>11</sup>:

$$\rho_j(\mathbf{k}) = \frac{1}{N_j} \sum_{l=1}^{N_j} \langle \text{Re} \{ \exp(i\mathbf{k}\mathbf{r}_l) \} \rangle ,$$

where  $\mathbf{r}_l$  is the coordinate of atom  $l$ ,  $\mathbf{k}$  is the fixed vector of the reciprocal lattice, the angular brackets denote averaging over all generated trajectories and  $N_j$  is the total number of atoms in a selected part of the sample. Vanishing of  $\rho_j$  means that a corresponding part of the crystal is melted and a long-range order in the atom disposition is absent. In the mentioned work,<sup>11</sup> the structure and self-diffusion along the boundary [001](310) $\Sigma 5$  in fcc material was studied. The thermal dependence of  $\rho_j$  suggests that a phase transition in the boundary occurs. It means that  $\rho_j$  decreases with the increase of temperature faster than the corresponding value for atomic planes far from the boundary (here the  $j$  index means an atomic plane in the boundary itself). Although extrapolation of the  $\rho_j$  value to the melting point of the crystal,  $T_m$ , yields zero (liquid), at lower temperatures the  $\rho_j$  remains finite. It signifies conservation of the long-range order on the boundary. At  $T = T_m$  the GB self-diffusion coefficient  $D$  is the same as for the liquid; however at  $T < T_m$  it is less than for the corresponding supercooled liquid. Based on these data the authors<sup>11</sup> confirm the fact that the boundary retains some order up to the crystal melting temperature and the most acceptable description is that of a GB structure in terms of increased concentration of point defects. In Refs. 12, 13, in contrast to Ref. 11, when simulating the boundaries  $\Sigma 5$  in Al bicrystal an decrease of  $\rho_j$  up to zero for atomic layers neighbouring the boundary was reported to be observed at about  $0.7 T_m$ .

J. Q. Broughton and G. H. Gilmer chose the other, "thermodynamic", approach to analyse the problem.<sup>14</sup> Neglecting the effects of interaction, a GB melts when twice the surface tension of a "crystal-melt" interface becomes less than that of the boundary. Having determined the frequencies of normal oscillations of atoms on the boundary at  $T=0$ , its entropy and thermal dependence of surface tension may be found. Then comparing it to the surface tension of a "crystal-melt" interface one may distinctly conclude whether this boundary is capable of melting or not. It should be remarked that such a conclusion is a qualitative one, since a thermal dependence of the boundary entropy is not taken into account. The authors<sup>14</sup> performed such an analysis for

the three boundaries: a) [001]  $\Sigma 5$  (310),  $\phi = 36.9^\circ$ ; b) [011]  $\Sigma 11$  (332),  $\phi = 20.05^\circ$ ; c) [011]  $\Sigma 123$  (443),  $\phi = 14.65^\circ$ . It appeared that the tendency of the boundaries to melt diminishes as long as the misorientation  $\phi$  decreases. Indeed, the MD investigation of the boundary behaviour at the temperature of a triple point demonstrated the fact that there is a thick disordered layer in the vicinity of the  $\Sigma 5$  boundary, this layer is significantly thinner near the  $\Sigma 11$  boundary and the boundary  $\Sigma 123$  remains ordered at this temperature.

It should be noted that the ordinary empirical potentials of a pairwise interaction of atoms fitted by several parameters (Morse, Lennard–Jones) were used in the above mentioned works.<sup>11–14</sup> However, such ordinary potentials describe adequately only the crystals of inert gases. In real metals a significant contribution to the pairwise interactions is made by the conduction electrons. For the present the most advanced account of this contribution is the embedded-atom potential. It is widely employed for simulation of defects in metals.<sup>15</sup> This potential allows for the change of local electronic density near the atom.

D. Wolf<sup>16</sup> was the first to use that potential for MD simulation of high-temperature behaviour of a GB. The twist boundary [001]  $\Sigma 29$  in Cu has been investigated. It appeared that up to  $T = 0.94 T_m$  the order parameter had a non-zero value in all atomic planes<sup>16</sup> adjacent to the boundary. Since it is the first work<sup>16</sup> where the embedded-atom potential was used and the  $\Sigma 29$  boundary is the large-angle boundary possessing high surface tension, the authors<sup>16</sup> confirm that GB melting is not the fact.

Analysing the results of the above mentioned experiments and simulations the following should be noted. A mere thermodynamic consideration shows that the coexistence of a crystal and equilibrium melt below the melting point  $T_m$  of a crystal is impossible.<sup>17</sup> In this respect GB melting is not possible. However a decrease of the temperature of “crystal-melt” equilibrium in a region neighbouring the boundary may occur if a melt is exposed to some external influence. Such an influence may take place as a result of interaction between the “crystal-melt” interfaces formed after GB melting. This interaction may have a complex character and change the structure of the liquid layer on the boundary. Recent investigations<sup>18</sup> of “crystal-melt” interface show that the melt “remembers” the disposition of atoms in a crystal at distances of up to 4–5 atomic layers from it. It is expressed by the peaks of the density profile in those sites where atoms must be positioned in a crystal. Now let us assume the following mental experiment: cut out from a bicrystal a flat piece, 8–10 interplanar spacings thick containing a GB and fill in the slit formed with melt. Such a layer will have a non-zero value of the order parameter  $\rho$  and retain the long-range order like in a crystal. Irrespective of this, such a layer may be described by the same state equation as for a liquid. Taking into account that the formation of very thick layers of liquid on the boundary is not likely (it is not favourable thermodynamically), the following scenario of GB melting may be presented (it is confirmed by the works<sup>10,11,16</sup>: with increase of temperature the order parameter  $\rho$  for the

boundary plane decreases permanently and goes to zero at  $T \Rightarrow T_m$ . At that temperature complete wetting of a boundary by its own melt is observed.

Note that in quite a number of theoretical works high temperature behaviour of various simplified models of GBs (e.g., the lattice-gas model,<sup>19,20</sup>  $q$ -state Potts model,<sup>21</sup> etc.) was investigated. The fact obtained was that a layer of liquid like phase occurs on the GB at a significantly lower temperature than the bulk melting point  $T_m$ . The layer grows logarithmically when approaching  $T_m$ . It is not clear, however, which of these models describe the behaviour of GBs in real material adequately.

The recent investigation of surface melting of lead has shown that liquid layer is not being formed on the low energetic faces (such as (001)).<sup>22,23</sup> Since the influence of the crystalline order on the interface structure is stronger in the case of GBs than in the case of external surface, it is obvious that GB melting in pure metals is rather doubtful.

In alloys the situation may be different. Fortunately, a variety of phase transitions in a solid is not limited by melting only. Therefore a situation may be assumed where a GB is substituted by the interlayer of another solid phase. Later we shall come back to this question once more.

#### 4. Other Types of Grain Boundary Phase Transitions

Since the GB is hidden inside a material, special efforts are required to observe it. Many results for boundary structure were obtained with the help of the thin film method.<sup>24</sup> Thin single-crystal films obtained, for example, with the aid of epitaxy on the surface of NaCl single crystals oriented in a proper manner are applied to each other and sintered. The thin film bicrystal obtained is investigated by means of a transmission electron microscope or by X-ray diffraction.

Sickafus and Sass using these methods found<sup>25</sup> a change of the dislocation structure of small-angle twist boundaries [001] in the bicrystals of a Fe-Au alloy when the content of gold was increased. In an iron bicrystal the dislocation grid consisted of dislocations with the direction  $\langle 110 \rangle$  and Burgers vector  $\mathbf{b} = (a/2)\langle 111 \rangle$ . After introducing a small amount of gold into a sample section consisted of dislocations with the direction  $\langle 100 \rangle$  and Burgers vector  $\mathbf{b} = a\langle 100 \rangle$  were found on the boundary.

Further Sass and Lean observed the change of dislocation structures, both small and large angle boundaries, in iron bicrystals with antimony impurity<sup>26</sup> and in those with sulphur impurity after ion implantation of sulphur.<sup>27</sup>

It is known that special GBs of arbitrary orientation are faceted; that is, they are divided into straight line sections with a special orientation. This is connected with the anisotropy of the boundary surface tension; the facets are located in those planes where the surface tension is minimal. A similar phenomenon is observed also on the surface of solids: many single crystals are of a faceted shape with flat sections corresponding to low-index crystalline faces which possess



extremely low surface tension. At a small deviation of a face orientation from a low-index one, steps occur on the surface and the energetically favourable orientation is partially conserved. In this case, however, the surface tension increases by an amount proportional to the free energy of the steps and their density (if the interaction between the steps is neglected). With increase of temperature the steps' contribution to the entropy increases, and at some temperature the formation of steps may become energetically favourable. Their spontaneous formation begins and their concentration becomes about 1. All the characteristic sizes at this stage are of interatomic distances. Transformation of atomically smooth surface into atomically rough one occurs; that is, a roughening phase transition takes place. It is obvious from what is said above that the surface tension of the rough surface must be isotropic and the crystal surface corresponding to such orientations must be of a rounded (non-faceted) shape.

In principle, the same phenomenon may be assumed also on the GBs. With a temperature increase, the boundary may become unstable with respect to introduction of steps and transforms into an atomically rough one. The surface tension of such a boundary must be isotropic, and macroscopically the transition is manifested in defaceting. The boundary becomes flat but somewhat diffuse.

It should be remarked that the diminishment of the respective quantity of faceted boundaries and a set of possible orientations of facets were observed several times in experiments on polycrystals during temperature growth (e.g. see Ref. 28). However, it is doubtful whether this effect is connected with the roughening transition or is of a kinetic nature. For a sufficient proof of the existence of such transition an experiment on the crystallographically certified single GB is required. Such an experiment has recently been performed by R. W. Balluffi *et al.*<sup>29</sup> In this work asymmetric tilt  $\Sigma 3\langle 111 \rangle$  boundaries in gold and aluminum and asymmetric  $\Sigma 11$  boundary in aluminum were obtained. At room temperature all such boundaries possessed a clearly defined facet structure. A direct observation of the boundaries upon heating inside an electron microscope demonstrated that with increase of temperature the facets gradually diffused and at high temperatures the boundaries became flat. On decreasing the temperature the boundaries became in possession of a facet structure again.

Note also that the reversible faceting/defaceting of GB in a copper film was observed under saturation/evaporation of bismuth.<sup>30</sup>

Structural changes on the GBs must be accompanied by a change of all their properties such as mobility, diffusion permeability, sliding rate along the boundaries, and so on. Therefore one may try to register a GB phase transition by observing the change of these properties. Watanabe *et al.*<sup>31</sup> investigated the temperature dependences of the GB sliding rate for the seven various symmetric tilt boundaries in zinc 99.999 at% pure and one boundary in a material 99.99 at% pure. For six of the seven investigated boundaries, knees were revealed at various temperatures  $T_c$ . It appeared that the  $T_c$  has a maximal value extremely close to the special misorientation  $\Sigma 9\langle 10\bar{1}0 \rangle$  and for the boundary with a misorientation

angle of  $16.5^\circ$  (the smallest of all the investigated misorientation angles) a knee was not observed at all. In a sample with increased content of impurity the  $T_c$  appeared to be higher by  $40^\circ\text{C}$  than that for purer samples. According to the authors the combination of all these results suggests the existence of a GB phase transition at the temperature  $T_c$ .

In Ref. 32 the ratio of the surface tension  $\sigma_1$  of the special boundary  $\Sigma 17$  in tin to that of the general type boundary  $\sigma_g$  with misorientation angle far from the special value  $\Sigma 17$  was studied. This ratio was defined for a triple junction formed at the contact of one special and two random (general) boundaries. In the investigated temperature range ( $0.85\text{--}1.0 T_m$ ) the temperature dependences of the ratio  $\sigma_1/\sigma_g$  demonstrated knees (see Fig. 2) which are characteristic features of a first order phase transition. In this work mobility of the same special boundaries was studied for the same temperature interval. For some boundaries abrupt decrease of mobility on increase of temperature was observed. The

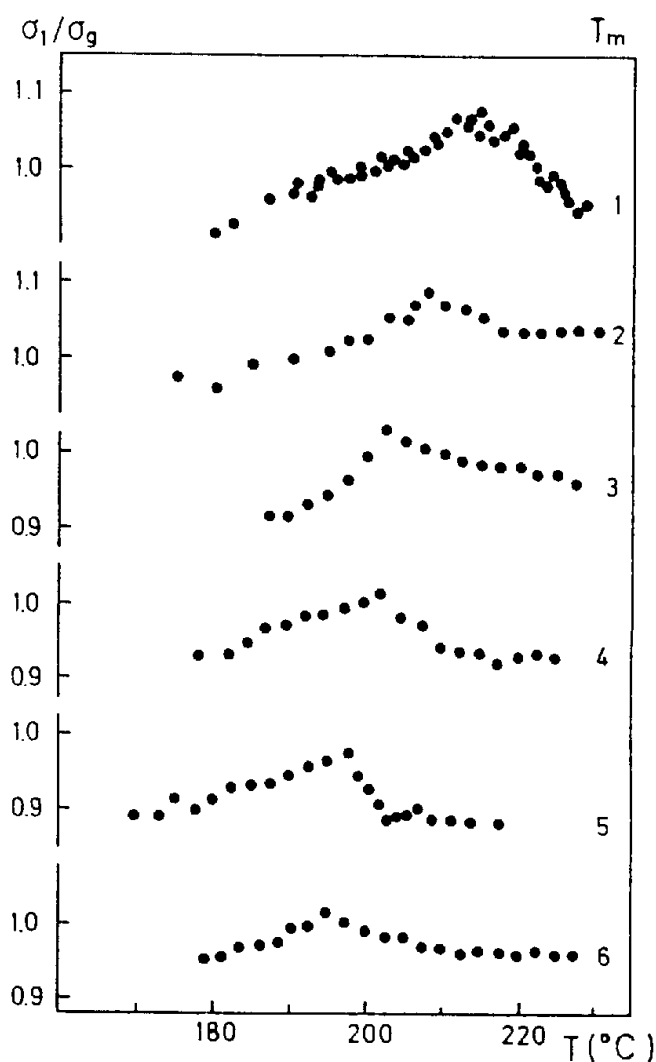


Fig. 2. Temperature dependences of relative surface tension  $\sigma_1/\sigma_g$  for the tilt boundary  $[100]$  in tin with misorientation angle  $\phi = 28.3^\circ$  and additional misorientation component of second tilt  $\theta_H$  (1 —  $\theta_H = 0^\circ$ ; 2 —  $3^\circ$ ; 3 —  $4^\circ$ ; 4 —  $5^\circ$ ; 5 —  $6.5^\circ$ ; 6 —  $9^\circ$ ).<sup>76</sup>

temperatures  $T_c$  at which abrupt change of mobility occurs are well coincident with the temperatures of the knees on the thermal dependences of the surface tension ratio. In Ref. 33 it was demonstrated that with an increase of the content of surface-active impurity in tin the temperature  $T_c$  decreases proportionally with the logarithm of impurity concentration.

To understand the dependences of the temperature of GB phase transition on impurity concentration and misorientation angle of grains, the surface analogy of the Clausius-Clapeyron relation is required. This relation connects the change of the phase equilibrium temperature with the change of other intensive thermodynamic variables. It may be obtained by means of the Gibbs adsorption equation written for both the GB phases<sup>34</sup>:

$$d\sigma = -S^p dT - \sum_i \Gamma_i d\mu_i + \hat{\xi} d\hat{n} , \quad (1)$$

where  $\sigma$  is the surface tension of a boundary,  $S^p$  is the surface excess of the boundary entropy (in a solution),  $\Gamma_i$  is the adsorption of the  $i$ th component on a boundary,  $d\hat{n}$  means a small change of the geometric macroscopic parameters of a boundary. For instance, if  $\hat{n} = \phi$ , then  $\hat{\xi} = \langle \partial\sigma / \partial\phi \rangle_{T,\mu}$ . At the GB phase transition point the surface tension of both the GB phases must be equal to each other (according to the condition of mechanical equilibrium). Thus one can obtain for a two-component alloy

$$(S_A^p - S_B^p)dT + (\Gamma_A - \Gamma_B)d\mu + (\Gamma'_A - \Gamma'_B)d\mu' + (\hat{\xi}_B - \hat{\xi}_A)d\hat{n} = 0 , \quad (2)$$

where  $A$  and  $B$  are the indices denoting the two different GB phases; the values with the primes refer to the atoms of a dissolved substance and those with the superscript  $p$  to the solution in general. Furthermore we shall consider a bulk solution to be ideal. Then

$$d\mu' = RTd(\ln c_v) + (R \ln c_v - S'_v)dT , \quad (3)$$

$$d\mu = -RTdc_v - (Rc_v + S_v)dT ,$$

where  $c_v$  is the bulk impurity concentration,  $S_v$  is the molar entropy in a bulk solution. Combining (2) and (3) we get the formula relating the temperature of a GB phase transition with the volume concentration of impurity, the values of adsorption on the boundaries, and the  $\hat{n}$  parameters:

$$dT = RT \frac{(\Gamma'_A - \Gamma'_B)d \ln c_v - (\Gamma_A - \Gamma_B)dc_v + [(\hat{\xi}_B^p - \hat{\xi}_A^p)] \frac{d\hat{n}}{RT}}{S_B^p - S_A^p - (\Gamma'_A - \Gamma'_B)(R \ln c_v - S'_v) + (\Gamma_A - \Gamma_B)(Rc_v + S_v)} . \quad (4)$$

Equation (4) is effective for analysing the experimental results. Following Ref. 32 let us consider the dependence of the GB phase transition temperature in pure tin on the misorientation angle of grains around the tilt axis [100]. For the estimation of surface excess values the specific area  $A$  occupied by one mole of GB substance must be known; the  $A$  values are different in different GB phases. To estimate them we assume the  $A$  value to be constant:

$$dT/d\phi \cong \frac{A}{\Delta S} ((\partial\sigma/\partial\phi)_B - (\partial\sigma/\partial\phi)_A) , \quad (5)$$

where  $\Delta S$  is the change of molar entropy of the GB substance under the phase transition:  $\Delta S = L/T_{tr}$ . In Ref. 32 the supposition was made that the peculiarities observed in the GBs' behaviour are connected with the phase transition "special GB-boundary of a general type". Indeed, the surface tension of a general type boundary depends weakly on the misorientation angle, therefore it may be assumed that  $(\partial\sigma/\partial\phi)_B \cong 0$ ; a change of the surface tension of a special boundary is connected with the elastic energy of the secondary GB dislocations wall:

$$\Delta\sigma_B = -\frac{Gb}{4\pi(1-\nu)} \sin(\Delta\phi) \left( 1 + \ln \frac{b}{2\pi r_0} - \ln(\Delta\phi) \right) . \quad (6)$$

Here  $r_0$  is the cutting radius which is approximately equal to the dislocations core width, and  $G$  and  $\nu$  are the elastic moduli. Combining (5) and (6) we obtain

$$\Delta T = -\frac{A}{\Delta S} \left[ \frac{Gb \sin(\Delta\phi)}{4\pi(1-\nu)} \left( 1 + \ln \frac{b}{2\pi r_0} - \ln(\Delta\phi) \right) \right] . \quad (7)$$

The heat of the GB phase transition,  $L$ , estimated in Ref. 32 from experimental data by means of Eq. (7), appeared to be close to the heat of pure tin melting, and the value  $r_0$  equals approximately  $5b$ . This confirms the assumption of the large width of SGBDs cores.<sup>35</sup>

The decrease of GB phase transition temperature in proportion to the logarithm of an impurity concentration is also elucidated in terms of Eq. (4) if the GB is assumed to be completely saturated with the impurity (all the adsorption sites are occupied). At this,  $\Gamma'_A$  and  $\Gamma'_B \cong \text{const}$  and  $dT \cong d \ln c_i$ .

As another example of the use of (4) consider the question: how does the rigid translation of lattices  $\mathbf{r}$ , breaking down the coincidence geometry on the boundary, affects the temperature of GB melting? A high temperature GB phase slides without any resistance, therefore  $\xi_B = (\partial\sigma/\partial\mathbf{r})_B \approx 0$  while  $(\partial\sigma/\partial\mathbf{r})_A > 0$ . Hence  $dT < 0$ , which means that upon the described shift a transition temperature decreases. Indeed, such decrease was actually observed in a recent work,<sup>36</sup> where the influence of the rigid shift on the GB premelting transition has being simulated on the basis of the lattice-gas model.

In the experiments of Watanabe<sup>31</sup> the temperature of a GB phase transition also decreased upon a deviation of the misorientation angle from the special value  $\Sigma 9$ . This proves the fact that the energy of a high temperature GB phase depends on the misorientation  $\phi$  more weakly than that of a low temperature phase. This is so because a high temperature phase is more disordered. However in this case there must be more adsorption sites on such a boundary and, according to (4), in a material with higher content of an impurity, the transition temperature must be lower. The fact that a contradictory situation is observed in the experiment indicates the possibility of occurrence of a non-equilibrium kinetic effect, instead of a phase transition. The similar effect expressed by abrupt changes on temperature dependences of GB migration velocity in zinc was reported in Ref. 37 and was connected with the breakaway of migrating GB from a cloud of adsorbed impurity.

## 5. Wetting Near Critical Point

We have discussed above the problem of GB melting and arrived at the conclusion that most probably it does not occur below the bulk melting point, while complete wetting of the GB by the melt at the melting point occurs. Wetting of GBs by the melt in two-component systems was actually observed (Zn–Sn,<sup>38,39</sup> Al–Sn,<sup>40–42</sup> Al–Pb,<sup>40</sup> Ag–Pb<sup>43</sup>). On the two-phase coexisting line and below the wetting temperature  $T_w$ , the contact angle at the intersection of a GB and the interface “solid–melt” is constant and roughly equals  $180^\circ$ . When  $T \Rightarrow T_w$ , this angle decreases rapidly and at  $T > T_w$  a melt layer appears on the GBs. So in a two-component material the problem of GB melting below bulk melting point transforms into the problem of whether or not a liquid (or quasi-liquid) layer occurs on a GB beyond the solid-liquid coexisting line.

It was J. W. Cahn<sup>44</sup> who first understood that in a two-component solution the transition from incomplete to complete wetting must always occur in the temperature vicinity of the critical point of immiscibility, and such a transition may have a “satellite” in the single-phase region prewetting or premelting phase transition. Consider a two-component liquid with miscibility gap  $\gamma + \beta$  which is in contact with a solid phase  $\alpha$  (cf. the phase diagram in Fig. 3a). The two-phase region is bounded by a dome-like curve with critical point  $c$ . Cahn showed that when  $T \Rightarrow T_c$  the surface tension  $\sigma_{\beta\gamma}$  of the interphase boundary between  $\beta$  and  $\gamma$  decreases faster than the difference between the surface tension values  $\sigma_{\alpha\gamma} - \sigma_{\alpha\beta}$ . This means that there exists a temperature  $T_p$  above which a layer of phase  $\beta$  between the container wall  $\alpha$  and the phase  $\gamma$  must exist. At temperature  $T_p$ , a wetting transition occurs on the conode  $PP$ . Cahn also showed that a thin thermodynamically equilibrium layer of phase  $\beta$  on the  $\alpha/\gamma$  boundary may exist even beyond the two-phase region on the phase diagram: between the  $PC''$ , line and the line bonding the region  $\beta + \gamma$ . When the line  $PC''$ , is crossed, prewetting transition occurs on the interphase boundary  $\alpha/\gamma$ : a layer of phase of finite thickness is formed abruptly.

Cahn's speculations are of a rather universal character and they allow one to make some very fruitful generalizations:

1. Wetting transition may occur even if the phases  $\beta$  and  $\gamma$  are solid. It is only important that  $\sigma_{\beta\gamma} \Rightarrow 0$  when  $T - T_c \Rightarrow 0$ .

2. For these phase transitions, the third phase  $\alpha$  is unnecessary. The layer of  $\beta$  may appear on GBs of phase  $\gamma$  if  $\sigma_{\gamma\gamma} > 2\sigma_{\beta\gamma}$ .

3. If the value of mixing enthalpy of components  $A$  and  $B$  is positive and large enough, then the critical point  $C$  may be "virtual". In other words, it may be situated, for example, above the liquid line of a two-component system (Fig. 3b). It is only important for wetting transitions that in the vicinity of such virtual point  $C$  the surface tension  $\sigma_{\beta\gamma}$  should decrease rapidly. Then we could observe, for example, the transition to complete wetting of GB by the melt.

In principle, the wetting phase may be solid. Actually, all the speculations which are true for the virtual decomposition curve (Fig. 3b), are true not only for the eutectic diagram, but also for the eutectoid one (Fig. 3c). Some data indirectly show that solid-phase wetting does exist. Such phase transition can exactly explain the stability of fine grains of the  $\gamma$ -phase in  $\beta$ -phase matrix in the two-phase ( $\gamma + \beta$ ) region for different superplastic alloys,<sup>45</sup> as well as the existence of the temperature threshold of GB plasticity enhancement.<sup>46</sup>

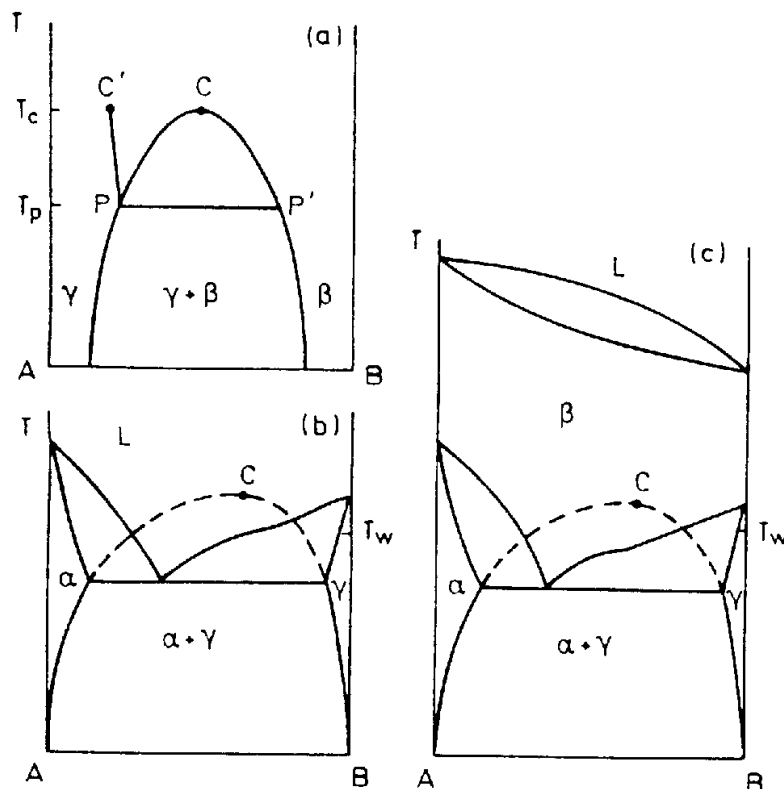


Fig. 3. a) The phase diagram for two-component liquid with miscibility gap. The wetting transition exists at  $T_p$  (by  $T > T_p$  the phase  $\beta$  wets the boundary between liquid phase  $\gamma$  and solid container  $\alpha$ ). Between  $PC'$  and  $PC$  lines the thin layer of phase  $\beta$  exists on the interphase boundary  $\gamma/\alpha$ . b) The eutectic phase diagram with virtual critical point  $C$ . The wetting transition on the  $\gamma/\gamma$  boundaries exists at  $T_w$ , near the temperature of little slope of liquidus line. c) The same situation as in the Fig. 3b, but for the eutectoid diagram. In this case by  $T > T_w$  the solid phase  $\beta$  must wet the grain boundaries  $\gamma/\gamma$ .

A similar interpretation was proposed by J. W. Cahn<sup>47</sup> for the experimental results on GB self-diffusion in Fe in  $\alpha$ - and  $\gamma$ -regions.<sup>48</sup> The step characteristic for first-order phase transitions was not observed in experiments on the thermal dependence of GB diffusion coefficient at the  $\alpha$ - $\gamma$  transition point. This can be connected with the solid  $\alpha$ -phase ability to wet the GBs in austenite.

As was mentioned above, GBs wetting by liquid metals in a two-phase region is a widely observed phenomenon. On the other hand, the theoretically predicted phase transitions accompanied by formation on GBs of thin layers of another phase in a single-phase region of the phase diagram (premelting, prewetting) has never been observed experimentally in solids. This may be explained in the following way. In systems for which the wetting of GBs by the melt was observed (Zn-Sn,<sup>38,39</sup> Al-Sn,<sup>40-42</sup> Al-Pb,<sup>40</sup> Ag-Pb<sup>43</sup>) the region of existence of solid solution based on the component with higher melting temperature is very narrow.

In the next part we will give an account of recent investigations of GB diffusion in Sn-In and Fe-Si-Zn alloys, the results of which may be treated in terms of prewetting and premelting phase transitions.<sup>49-52</sup> In the study<sup>49</sup> a critical point of the  $\gamma'$ - $\beta$  transition, approximately at  $T_c \cong 179^\circ\text{C}$ , has been revealed (cf. Fig. 4). The difference in structure of  $\beta$  and  $\gamma'$  phases is small and the two-phase regions  $\beta + \gamma'$  on the phase diagram are very narrow.

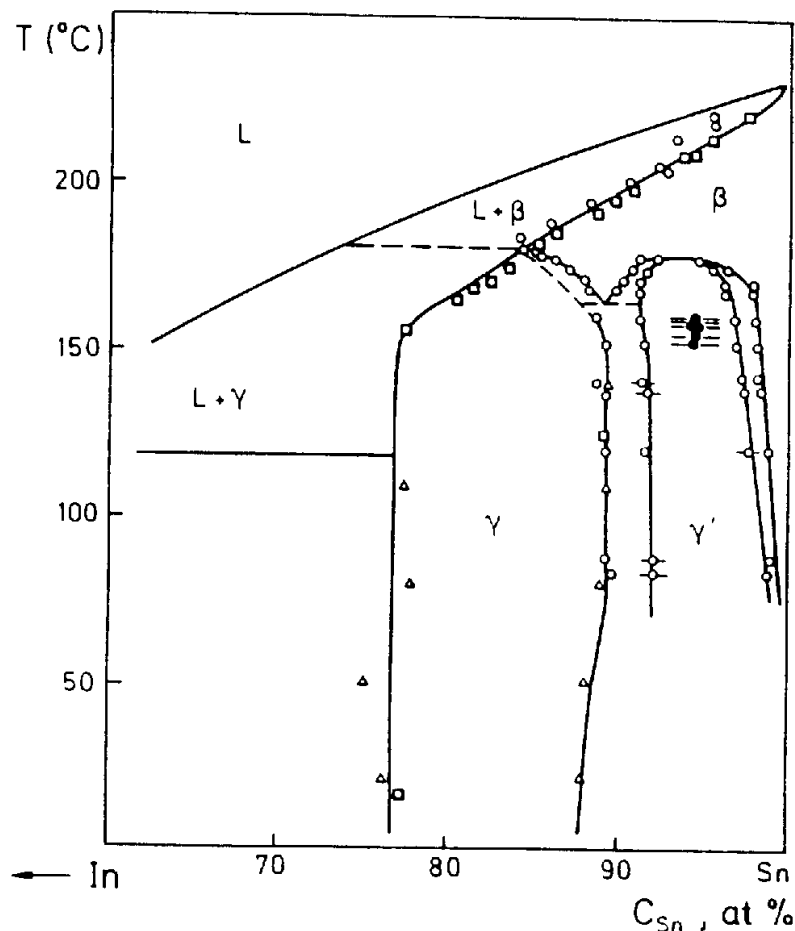


Fig. 4. The Sn — rich part of Sn — In phase diagram. The solid points show the temperatures of  $\gamma'$ - $\beta$  transition on grain boundaries (the rupture temperatures on the diffusion curves, see Fig. 7).<sup>49</sup>

Fe–Zn the line of solubility limit in the solid solution based on the bcc-iron is placed very near to the metastable curve of solid solution decomposition, and the “virtual” critical point of this curve lies only a little above the peritectic temperature.<sup>53,54</sup> According to Ref. 44 such systems are appropriate candidates for GB wetting. On the other hand, the region of existence of Fe-based solid solution in a Fe–Zn system and the homogeneity region of  $\gamma'$ -phase in a Sn–In system are large enough for the registration of changes in GBs' properties at prewetting or premelting transition. In order to study such changes in GB kinetic properties, parameters of GB and the bulk interdiffusion of Zn and Fe in a Fe–Zn–Si system,<sup>51,52</sup> and that of Sn and In in a Sn–In system<sup>49,50</sup> have been measured. In our further discussion we will distinguish two possible situations: first when a layer of new phase is formed on GB (prewetting transition), and, second when the GB is replaced by the layer of a new phase (premelting phase transition) (Fig. 5). At prewetting transition the difference between the two phases must be small, while at premelting transition the wetting phase may differ from that of the bulk dramatically. So a Sn–In system may demonstrate the GB prewetting transition, while in a Fe–Zn system one can observe the GB premelting transition.

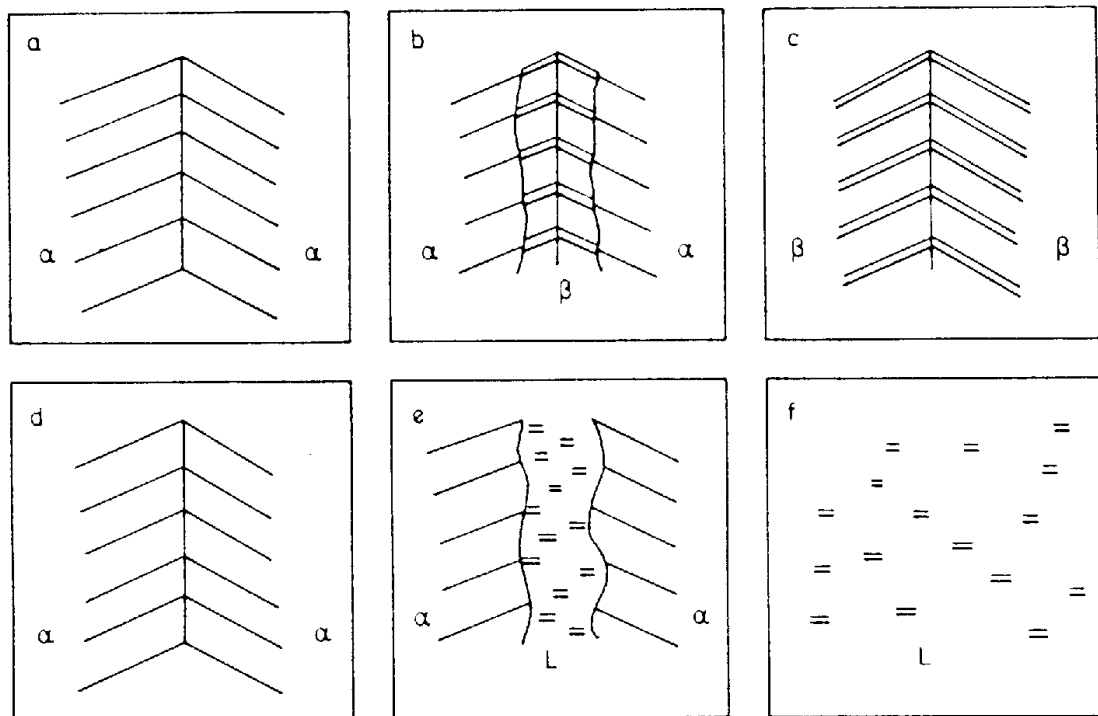


Fig. 5. a–c) prewetting transition; a — the grain boundary in  $\alpha$ -phase; b — the grain boundary in the thin quasi- $\beta$  layer between two  $\alpha$ -crystals near the bulk  $\alpha$ - $\beta$  transition; c — the grain boundary in  $\beta$ -phase; d, e, f — premelting transition; d — the grain boundary in  $\alpha$ -phase; e — the thin liquid layer between two  $\alpha$ -crystals near the solid–liquid coexistence line; f — the liquid by  $T > T_m$ . At the prewetting transition three interfaces are forming instead of the single grain boundary: new grain boundary and two “crystal-wetting phase” interfaces. At the premelting transition the grain boundary is completely replaced by the wetting phase interlayer.



## 6. Diffusion as a Tool for Investigation of Phase Transitions

The diffusion coefficient is very sensitive with respect to crystal structure. On the other hand, GB diffusivity measurements allows one to separate properties of the thin boundary layer from the crystal bulk properties. So such measurements may be applied to the investigation of phase transitions on GBs.

To determine the coefficient of GB diffusion, a model is necessary which would provide the opportunity to calculate the coefficient from the bulk concentration profile formed by impurity diffusion from the GB. From such models, Fisher's model is the simplest, being at the same time relevant to the experimental conditions. Forty years have passed since the publication of the paper formulating this model,<sup>55</sup> but it was so fruitful that even now it serves as the basis of most of the GB diffusion coefficient measuring methods. In this model, a GB is assumed to be a plate of thickness  $\delta$  with diffusion coefficient  $D'$ , several orders of magnitude higher than the bulk diffusion coefficient  $D$ . The impurity diffuses from a surface layer, and then leaks from the GB into the bulk. It is also assumed that diffusion in neighbouring bulk layers of different depths occurs independently. Direct diffusion from the surface into the bulk is also neglected. The bulk diffusion coefficient is assumed to be independent of the concentration  $c$ . Under these assumptions Fisher<sup>55</sup> derived an approximate equation for the impurity concentration distribution in the  $x-y$  plane, perpendicular to the GB and the sample surface,

$$c = c_0 \exp[-(4D/\pi t)^{1/4} y (D' \delta)^{-1/2}] (1 - \operatorname{erf}(x/2\sqrt{Dt})) \quad (8)$$

It should be noted that the mean square displacement of the impurity atoms along the GB is  $\langle x^2 \rangle \cong t^{1/4}$ . This law is also valid for diffusion along the infinite two-dimensional comb,<sup>56</sup> which is often used as a simple model of diffusion in disordered media.

For practically, determining the GB diffusion coefficient, the logarithm of the maximum impurity concentration on the GB  $c_b$  ( $x=0$ ) is plotted against the depth  $y$ . Such plots are termed Fisher dependences below. These are straight lines, whose slope corresponds to the value of the product  $D'\delta$ . The expression (8) has been modified many times later (see, for example, Ref. 57). Fisher's method has been shown to yield satisfactory results, if the Le Claire criterion  $\beta_{1c} = D'\delta/D\sqrt{Dt} \gg 1$  is observed. In the experiments discussed in Refs. 49–52 its value was equal to  $10^1 \dots 10^2$ , so the application of (8) was correct.

Now we shall discuss how a phase transition can affect the interdiffusion coefficient  $D$  that was determined in Refs. 49–52. According to the Darken theory,<sup>58</sup>

$$D = (c_a D_b^* + c_b D_a^*) g \quad (9)$$

Here  $D_a^*$  and  $D_b^*$  are the self-diffusion coefficients of the components,  $g = \frac{c_a c_b}{kT} \times \frac{\partial^2 F}{\partial c^2}$  is the thermodynamical factor, and  $F$  is the free energy per particle of the alloy. The values of  $D_a^*$  and  $D_b^*$  depend upon the length of diffusion jump, frequency of the atomic oscillations, and the vacancy formation and migration free energy. Therefore, two possible causes of  $D$  change during a phase transition can be envisaged:

1. Change of the parameters determining  $D_a^*$  and  $D_b^*$ .
2. Change of the thermodynamical factor  $g$ .

When a first-order phase transition occurs, the first cause is the most important one and the diffusion coefficient is changed by a finite value. Here the temperature dependence of  $D$  must undergo the rupture. For second order phase transitions, the second factor is more important than the first one. Change of  $g$  can lead to the appearance of a rupture or a  $\lambda$ -anomaly on the temperature dependence of  $D$ . Besides, if the diffusion coefficient is related to a critical mode (e.g., it corresponds to the order parameter relaxation near the phase transition point), then a group of atoms of size  $\cong \xi$  (correlation length) can move as a single whole. Here the diffusion mechanism is changed, which is accompanied by a dramatic growth of  $D$  ( $\lambda$ -anomaly). Consider this aspect in greater detail, following Ref. 59. Landau series expansion for  $F(c, T, \eta)$ ,  $\eta$  being the order parameter, has the form

$$F = F_0(c, T) + A(c, T)\eta^2 + B(c, T)\eta^4 + \dots$$

Here  $A(c, T) = a(T - T_c(c)) = a_1(c - c_c(T))$ . Because the system is far from the critical point where  $\partial T_c / \partial c = 0$ , the parameters  $a$  and  $a_1$  are related by  $a_1 = a(\partial T_c / \partial c)$ . The value of  $g$  can be obtained directly from the functional minimum condition  $\partial F / \partial \eta = 0$  which yields  $\eta^2 = a_1(c_c - c) / 2B$ :

$$g = (\partial^2 F / \partial c^2) \frac{c(1-c)}{kT} = \begin{cases} ((\partial^2 F_0 / \partial c^2) - a_1^2 / 2B)c(1-c) / kT, & \eta > 0, \\ (\partial^2 F_0 / \partial c^2)c(1-c) / kT, & \eta = 0. \end{cases}$$

Therefore, we see that the thermodynamical factor (and consequently the interdiffusion coefficient) undergoes a finite jump in a second-order phase transition.

This behaviour certainly changes in the fluctuation region, where the Landau theory ceases to be valid. To study these changes, the scaling hypothesis can be used.<sup>60</sup> According to this hypothesis, the free energy  $F$  must be expressed as

$$F \cong \xi^{-d},$$

$\xi$  being the correlation radius of the system, and  $d$  the system dimensionality ( $d = 2$  or  $3$ ). But  $\xi \cong |T - T_c|^{-\nu}$ , where  $\nu$  is the critical index of the correlation

radius. Then,  $g \cong (\partial_2 F / \partial c^2)_T \cong |c - c_c|^{vd-2}$  because  $|T - T_c| \cong |C - C_c|$ . Here  $vd - 2 = \alpha$ ,  $\alpha$  being the critical index of specific heat. The absolute value of  $\alpha$  is usually rather small ( $\cong 0.1$ ), but can be either negative or positive. If  $\alpha < 0$ , then the diffusion coefficient can grow to infinity in the vicinity of a phase transition. It should be noted that here we mean the  $\alpha$  index measured at a fixed concentration, rather than the  $\alpha$  index measured at a fixed chemical potential. Other works mostly deal with  $\alpha$ .

The anomalous growth of the diffusion coefficient was observed experimentally in Ref. 61. In this work, diffusion of sub-monolayer barium film on molibdenium (110) face was studied. Here, the behaviour of the diffusion coefficient  $D$  was found to be strongly correlated with the surface structure of the film. At concentrations corresponding to the formation of two-dimensional lattices  $C(6 \times 2)$  and  $C(2 \times 2)$ , the diffusion coefficient grew drastically while the activation energy decreased. The growth of the diffusion coefficient is revealed by the appearance of a plateau on the barium surface concentration profile. In Ref. 62, the mass transfer was supposed to occur on account of the motion of the solitons in the incommensurate phase. Since, by this assumption, the mass transfer is contributed by all adatoms on the soliton line, the diffusion coefficient grows. The authors of Ref. 59 stress that this growth may also be connected with the anomalous behaviour of  $g$ .

All the above consideration confirms that diffusion is an adequate and sufficiently sensitive tool for investigation of GB phase transitions.

## 7. Premelting Transition at Grain Boundaries in Alloys

A work<sup>49</sup> devoted to studies of the behaviour of GBs in Sn–In alloy in the vicinity of the critical point of  $\beta - \gamma'$  transition (see Fig. 4) was carried out on tin bicrystals with twist GBs [001]. Four GBs of the studied samples belonged to the region of existence of special GB  $\Sigma 17$ ,<sup>32</sup> their structure containing secondary GB dislocations. The fifth GB was a general large-angle GB. The  $\beta$ -phase is transformed into  $\gamma'$ -phase by shifting one of the bct sublattices of  $\beta$ -tin along the tetragonal axis  $c$ .<sup>63</sup> This is why the choice of twist GB [001] would ensure avoidance of change of the CSL geometry during the bulk  $\beta - \gamma'$  transition. The paper<sup>50</sup> was devoted to investigations of four [001] twist tin-germanium interphase boundaries with different misorientation angles. Three of the four interfaces were inside the region of existence of epitaxial interphase boundary  $\Sigma 1$ .<sup>64</sup> The technique of growth of tin bicrystals is reported in detail in Ref. 32, while Ref. 64 is devoted to the same for tin-germanium bicrystals. Below we present the results of studies of indium diffusion by these boundaries (according to Refs. 49, 50).

The temperature dependence of the interdiffusion coefficient of indium in tin in indium concentration range 2 through 8 at% is shown in Fig. 6. This dependence undergoes a rupture at  $T_c = 178.7 \pm 0.5^\circ \text{C}$ . Both above and below

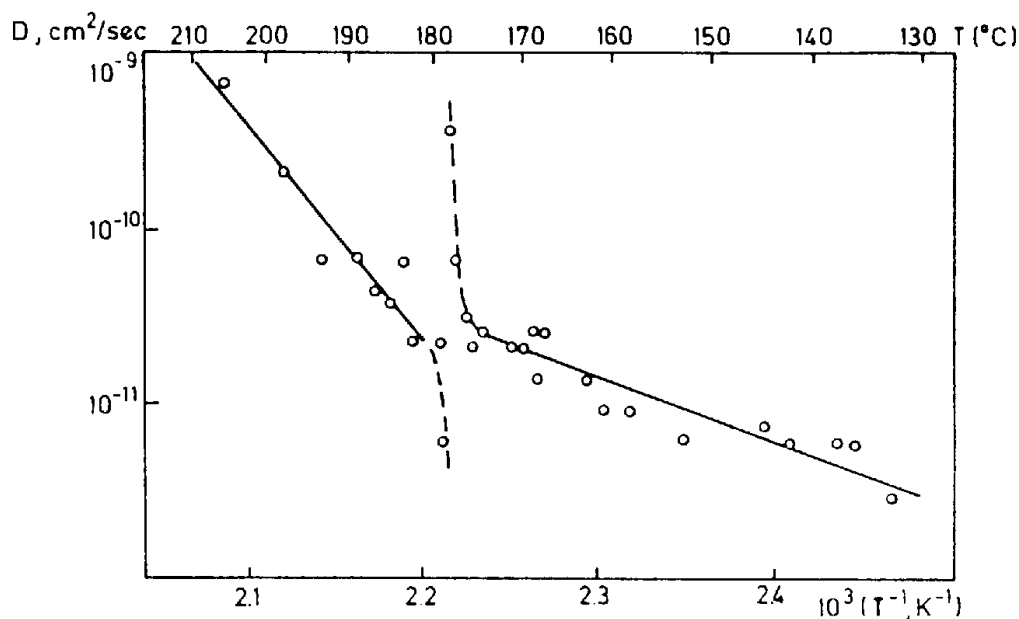


Fig. 6. The temperature dependence of indium bulk interdiffusion coefficient  $D$  in tin. The discontinuity on the temperature dependence at  $T_c$  corresponds to the critical point of the  $\beta$ - $\gamma'$  transition (see Fig. 4). Deviations from the Arrhenius law near  $T_c$  are seen.<sup>49</sup>

this point, the dependence is in agreement with the Arrhenius law. The value of  $T_c$  coincides with the temperature of  $\gamma'$ -phase precipitation from In solid solution in  $\beta$ -tin (see Fig. 4). When  $T_c$  is approached from the higher temperature region,  $D$  values are shifted down from the Arrhenius curve, this shift being the opposite if  $T_c$  is approached from the lower temperature region. The GB diffusion coefficients, as well as the  $D$  values for bulk diffusion, were determined in concentration range 2 through 8 at% of indium. Figure 7 displays the temperature dependences of the product  $D'\delta$  of five studied twist GBs with different misorientation angles. On each of these dependences, two regions can be observed: the high-temperature and the low-temperature ones. The diffusion coefficient changes abruptly at a temperature  $T_c^b$ . Different interfaces are characterized by different  $T_c^b$  values. All these values are lower by 17 to 25° C than the  $T_c$  value for bulk diffusion coefficient. The temperature dependences of  $D'\delta$  do not exhibit any singularities at the temperature of bulk  $\beta$ - $\gamma'$  transition  $T_c$ , where  $D$  undergoes a rupture. The temperature dependences of the product  $D'\delta$  for four studied twist tin-germanium interphase boundaries are presented in Fig. 8. On each of these dependences a rupture is observed at a temperature  $T_c^b$ . The values of this parameter for different interfaces is again different. The values of  $D'\delta$  presented in Fig. 8 (as well as in Figs. 6, 7), correspond to In concentration in the range from 2 to 8 at%.

All temperature dependences of  $D'\delta$  shown in Fig. 8 exhibit deviations from the Arrhenius law near  $T_c^b$ . When  $T_c^b$  is approached from the region of lower temperatures, the values of the diffusion coefficient are higher than they should be according to the Arrhenius law, while on the other side of  $T_c^b$  the situation

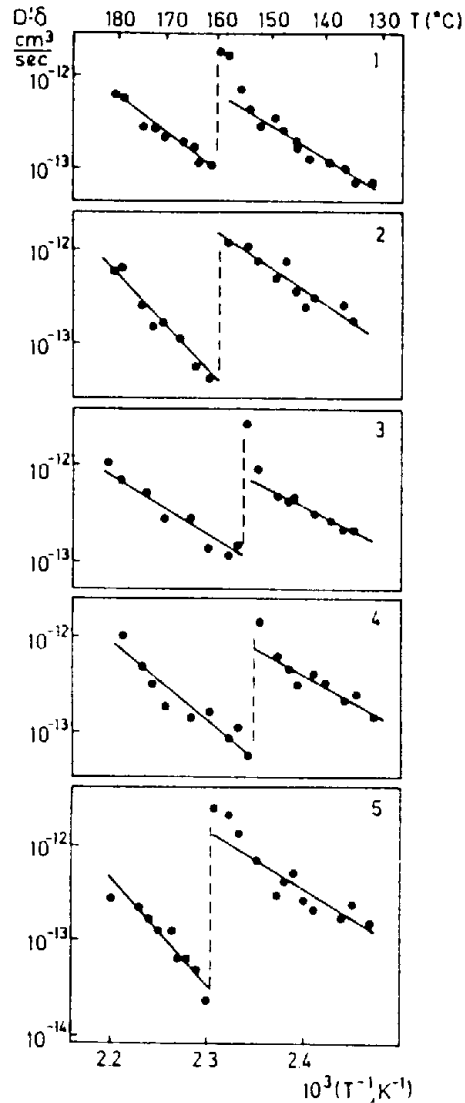


Fig. 7. The temperature dependences of the product of the grain boundary diffusion coefficient of indium  $D'$  and the boundary width  $\delta$  for [001] twist boundaries in tin with different misorientation angles  $\phi$ : 1 — 28.1°; 2 — 29.1°; 3 — 27.6°; 4 — 30.2°; 5 — 31.1°.<sup>49</sup>

is the opposite. The deviations are observed in the temperature of approximately  $T_c^h \pm 5^\circ \text{C}$ . Such behaviour of the diffusion coefficient is probably due to the critical phenomena in the vicinity of a phase transition on a GB and in the bulk.

The anomalous behaviour of GB diffusion coefficient can be discussed in terms of GB prewetting transition (see Fig. 5). Suppose that an interlayer of high-temperature  $\beta$ -phase is formed at temperature  $T_c^h$  on the GBs and interphase boundaries in low-temperature  $\gamma'$ -phase. As the temperature is further increased, the thickness of this interlayer also grows, the structure of the GB itself becoming analogous to the  $\beta$ -phase GB structure, rather than to that of the  $\gamma'$ -phase. The thickness of this layer approaches infinity at the temperature of bulk transition

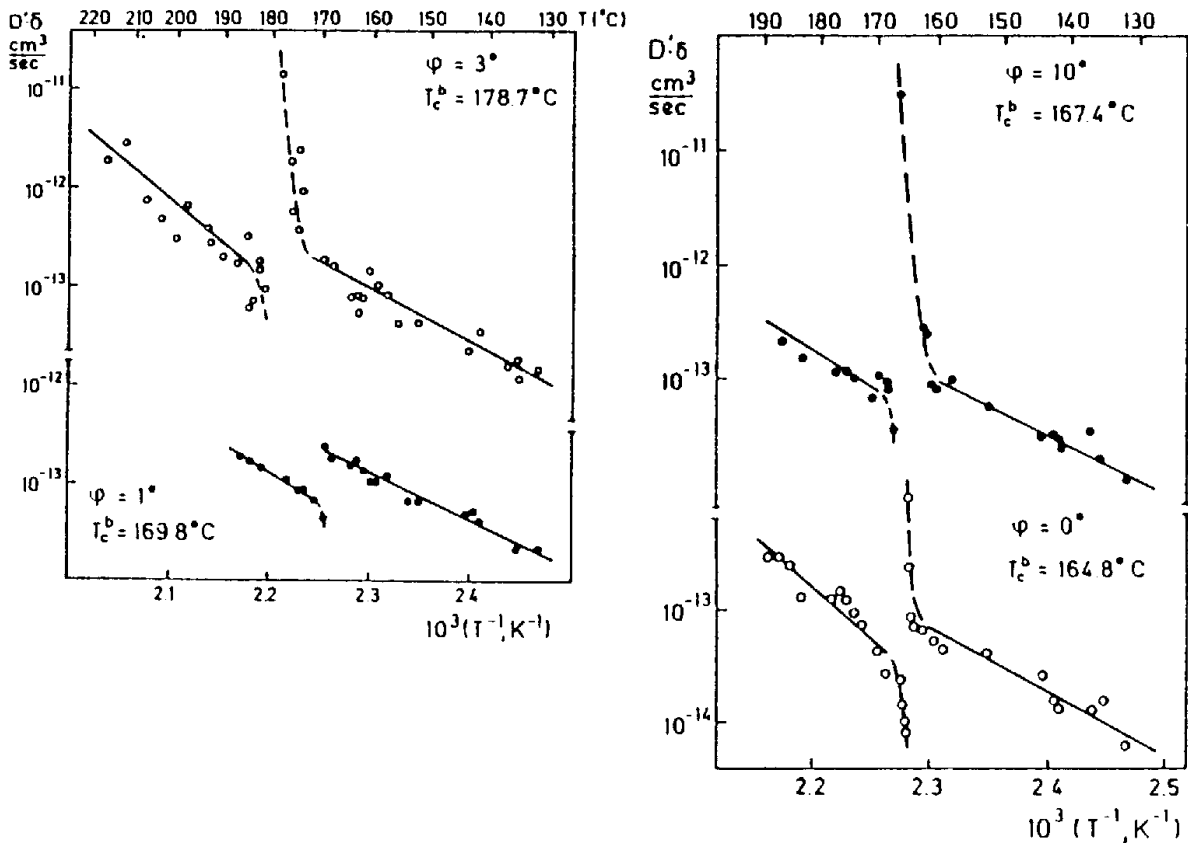


Fig. 8. The temperature dependences of the product of the boundary diffusion coefficient of indium  $D'$  and the boundary width  $\delta$  for four [001] twist Sn-Ge interphase boundaries. The misorientation angles and temperatures of the  $\beta$ - $\gamma'$  phase transitions on the boundaries are shown.<sup>50</sup>

$T_c$ , but this, indeed, does not affect the structure of a GB. This is why the temperature dependences of GB diffusion coefficients have no singularities at  $T_c$ .

The dependence of  $T_c^h$  upon the misorientation angle is plotted in Fig. 9. The temperature can be seen to decrease with the increase of deviation of the misorientation angle from the coincidence misorientation  $\phi_{\Sigma 17} = 28.1^\circ$ . The  $T_c^h$  value decreases within the region of existence of special GBs  $\Sigma 17$ . Outside this region,  $T_c^h$  grows. The difference between the bulk temperature  $T_c$  and the GB temperature  $T_c^h$  is also presented in Fig. 9.

Figure 10 illustrates the dependence of the  $T_c^h$  for interphase boundaries on the  $(\phi - \phi_\Sigma)$  value. Here  $\phi$  is the misorientation angle of the studied interphase boundaries, while  $\phi_\Sigma$  denotes the angle corresponding to the minimal surface tension of tin-germanium interfaces and extremal diffusion parameters.<sup>64</sup> The transition temperature is maximal for  $(\phi - \phi_\Sigma) = 0$ . It decreases with the growth of the deviation from the angle  $\phi_\Sigma$ . The  $T_c^h$  value for tin GBs also decreases when moving away from the coincidence misorientation  $\Sigma 17$ . The point corresponding to the general boundary with misorientation angle  $10^\circ$  ( $(\phi - \phi_\Sigma) = 7^\circ$ ) is also above the straight line extrapolated from the region of existence of special GBs.

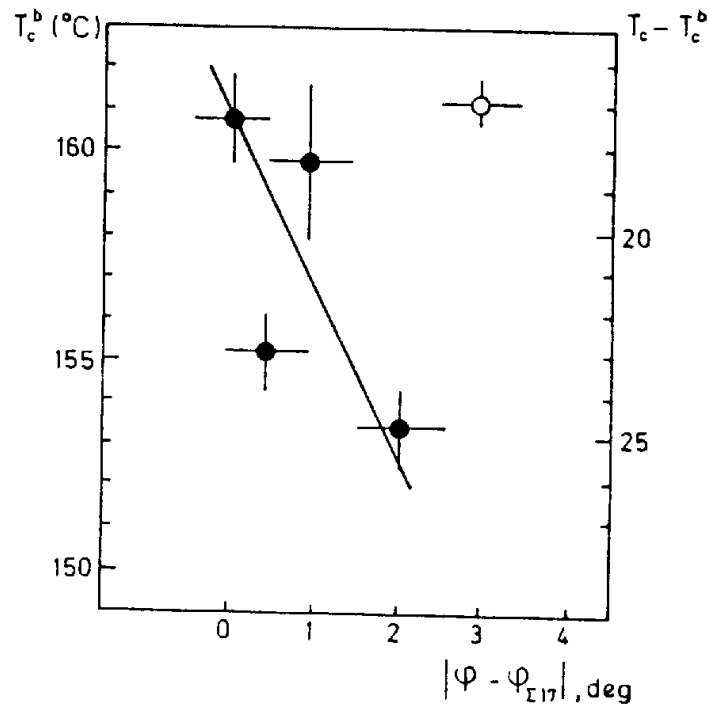


Fig. 9. Dependence of the  $\beta$ - $\gamma'$  transition temperature  $T_c^b$  on the grain boundaries in tin on the misorientation angle  $\phi$ .  $T_c$  is the temperature of the critical point of the  $\beta$ - $\gamma'$  transition in the bulk. (●) boundaries lying within the region of existence of special boundaries  $\Sigma 17$ , (○) a general boundary,  $\phi_{\Sigma} = 28.1^\circ$  ( $\Sigma 17$ ).<sup>49</sup>

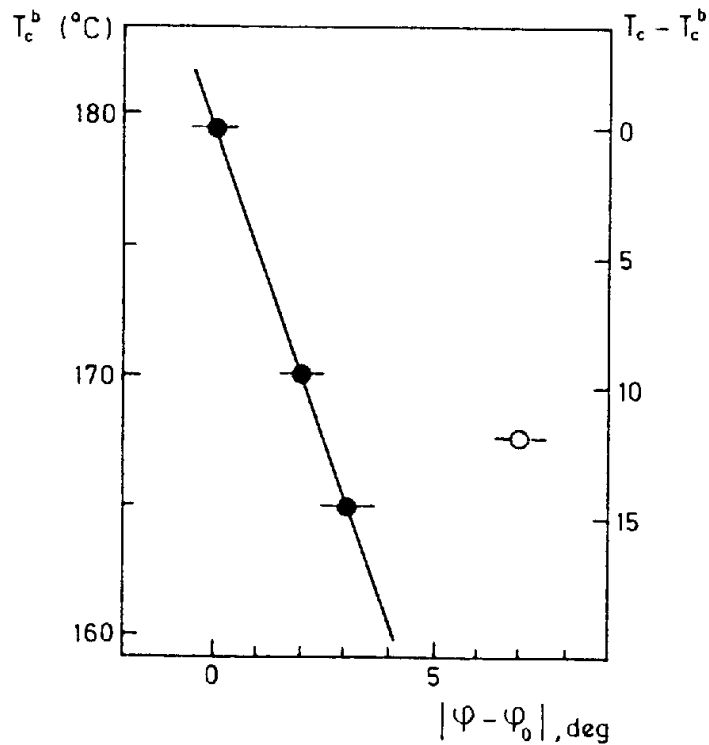


Fig. 10. The misorientation dependence of the  $\beta$ - $\gamma'$  phase transition temperatures on the twist [001] Sn-Ge interphase boundaries;  $\phi_0 = 3^\circ$ , at  $\phi = 3^\circ$  the interphase boundaries possess the minimum surface tension and extreme properties;  $T_c$  the temperature of the critical point of the  $\beta$ - $\gamma'$  transition in the bulk; ● — special boundaries; ○ — general boundary.

The same deviation is observed for general GB in tin. Figure 10 also presents the difference between the bulk and GB transition temperatures  $T_c^b - T_c$ . Its value changes from 0°C to 14°C.

What can serve as the cause for the observed misorientation dependence of GB transition temperature? The  $\gamma$ -phase of Sn-In alloy has simple hexagonal lattice. It can be produced from  $\beta$ -tin lattice by shifting one of the sublattices along the tetragonal axis  $c$  by 1/4 period with consequent slight deformation. For  $\gamma'$ -phase, the said shift should be performed by a distance smaller than  $c/4$ . If the alloy state is described by the order parameter  $\eta$  proportional to the magnitude of such a shift, the problem will become equivalent to that of wetting of a solid substrate by fluid. This problem has been treated in detail in the review.<sup>65</sup> Here, zero value of  $\eta$  corresponds to the high temperature, symmetrical structure of  $\beta$ -tin, non-zero  $\eta$  values corresponding to the low-temperature, non-symmetrical  $\gamma'$ -phase. Due to the distorting influence of a GB, the order parameter values  $\eta'$  in the atomic layers adjacent to the GB differ from the alloy bulk value  $\eta$ .

However, if the prewetting hypothesis is true, we should have  $\eta' = 0$  for  $T > T_c^b$  and  $\eta' \neq 0$  for  $T < T_c^b$ .

As it has been shown above, a grid of the so-called secondary GB dislocations (SGBDs) appears on special GBs slightly (by a small  $\Delta\phi$ ) deviated from the coincidence misorientation  $\phi_\Sigma$ . The period of such a SGBD grid is given by  $d = b/2\sin(\Delta\phi)$ . Consider the simplest assumption that the SGBD core structure corresponds to that of high-temperature symmetrical GB phase. In this assumption, the following functional (corresponding to the mean-field theory) should be minimized:

$$\Phi_B = \int_0^d \{0, 5(\partial\eta'/\partial x)^2 + \Phi(\eta')\} dx \quad (10)$$

with the boundary conditions

$$\eta'(0) = \eta'(d) = 0; \quad \partial\eta'/\partial x|_{x=0} = \partial\eta'/\partial x|_{x=d} = 0 \quad (11)$$

Here,  $\Phi(\eta')$  is the thermodynamical potential of a unit volume of the GB phase corresponding to the special misorientation  $\Sigma$ <sup>17</sup>. This function has two minima below  $T_{\text{csp}}^b$ , the minimum for  $\eta' = 0$  surpassing the minimum for  $\gamma'$  phase by the value of the ‘‘thermodynamical gap’’  $\Delta$ .

Considering (10) with (11), one finds that the phase transition (caused by nullification of  $\eta'$ ) is shifted towards the higher-temperature region for the GB with dislocations as compared with the purely special boundary. The magnitude of such a shift is

$$\Delta T = T_c^{\text{sp}} - T_c^b \cong \Delta \cong d^{-1} \cong |\Delta\phi| \quad .$$



Therefore, when the misorientation angle of a GB is deviated from the coincidence misorientation  $\phi_\Sigma$  by a small  $\Delta\phi$ , the GB prewetting temperature decreases in proportion to  $\Delta\phi$ . When  $\Delta\phi$  is so large that the GB is outside the region of existence of the special GB, such a GB will have no large-scale inhomogeneities. On such a GB, prewetting transition will occur at a higher temperature than on special GB with close misorientation angle. These considerations provide qualitative explanations to the experimental dependences of  $T_c^h(\phi)$  obtained in Refs. 49, 50.

Therefore, the model of prewetting transition answers the following questions:

1. Why the ruptures on the temperature dependences of the GB diffusion coefficient are observed at all dependences.
2. Why the GB transition temperatures are below the bulk one.
3. Why the temperature dependences of GB diffusion coefficients have no singularities at the bulk transition temperature.
4. Why the temperature of GB transition grows with the increase of deviation of the misorientation angle from the special value.

However, two important facts distinguish the behaviour of GBs from that of interphase boundaries. First, the transition temperatures on all interphase boundaries are higher than on GBs. We think that this can be qualitatively understood within the framework of the lattice-gas model proposed by Pandit<sup>66</sup>: the adatoms occupy the sites of a uniform lattice filling the infinite region  $z > 0$ , the nearest neighbours interact with a potential of amplitude  $V$ . The substrate attracts all adatoms in the nearest adsorption layer, the attraction potential being equal to a constant  $U$ . Applying Landau theory to this model, one can show that for  $U/V > 1$  the interaction with the substrate is so strong that it is wet at temperatures as low as  $T = 0$ . With  $U/V$  in the range from 0.7 to 0.9, the system undergoes a first-order wetting transition (and, consequently, a first-order prewetting transition) at  $T_w > 0$ . When the interaction with the substrate is further decreased,  $T_w$  grows up to  $T_c$ , and in the range  $0.5 < U/V < 0.7$  critical wetting is observed. Therefore, the chance to obtain second-order wetting increases as fluid interaction with the substrate weakens. Since mutual solubility in solid state is practically absent in the system Sn–Ge, the potential  $U$  of Sn atoms interacting with Ge must be far lower than the pair potentials Sn–Sn or Ge–Ge. On the other hand, if we consider a grain as a set of atoms adsorbed on the substrate formed by a second grain, we shall find that the potential  $U$  is comparable with the tin atomic interaction potential  $V$ .

So, the  $U/V$  value is higher for GBs than for interphase boundaries. According to the results obtained by Pandit *et al.*, it means that the temperature of wetting transition (as well as that of the associated prewetting transition in the single-phase region) must be higher for the interphase boundaries. The transition itself for the latter must be closer to a second-order one, with strongly developed critical phenomena. This has all been observed experimentally.<sup>49,50</sup>

## 8. Critical Behaviour of Grain Boundary Diffusion Parameters in the Vicinity of Prewetting Transition

As has already been said, such unusual behaviour of indium diffusion coefficient along the tin-germanium interphase boundaries in the vicinity of the GB phase transition can be related to either the behaviour of the thermodynamical factor  $g$  or the change of the diffusion mechanism. Consider both of these in greater detail.

The region of homogeneity of  $\gamma'$ -phase on the Sn–In phase diagram is separated from the region of  $\beta$ -phase homogeneity by two two-phase regions (see Fig. 4). This means that the concentration dependence of alloy free energy  $F$  must have three minima, so the  $F(C)$  dependence can be represented as a sixth power polynomial. We can write the following equation:

$$F = F_0(T) + A(T)(C - C_c)^2 + B(T)(C - C_c)^4 + D(T)(C - C_c)^6 . \quad (12)$$

Here,  $c_c$  is the indium concentration at the top of the  $\gamma'$ -phase “dome”. At this point the conditions  $A(T_c) = 0$ ,  $B(T_c) = 0$  should be satisfied. Similarly to the Landau theory, we limit our expansion by the linear term

$$A(T) = \alpha |T - T_c| .$$

Then, taking into account that the interdiffusion coefficient is measured in a concentration range near  $c_c$ , we obtain

$$\partial^2 F / \partial C^2 |_{C=C_c} = 2\alpha |T - T_c| .$$

If the phase diagram of the interphase boundary does not differ significantly from the bulk one for Sn–In system, then one can similarly write:

$$\partial^2 F / \partial C^2 |_{C=C_B} = 2\alpha_B |T - T_c^b| .$$

So, taking (9) into account, we can estimate  $D$  as follows:

$$\ln D \sim \ln |T - T_c^b| .$$

Consequently, when  $T_c^b$  is approached from the higher temperature region, the diffusion coefficient approaches zero as  $|T - T_c^b|$ . This means that the critical index of the diffusion coefficient in the vicinity of  $T_c^b$  must be equal to unity when  $T \Rightarrow T_c^b + 0$ .

Figure 11 presents the dependence of the indium diffusion coefficient along the twist tin-germanium interphase boundary with misorientation angle  $0^\circ$  on the parameter  $|T - T_c^b / T_c^b|$ . The dependence is plotted in log-log coordinates.<sup>50</sup> As

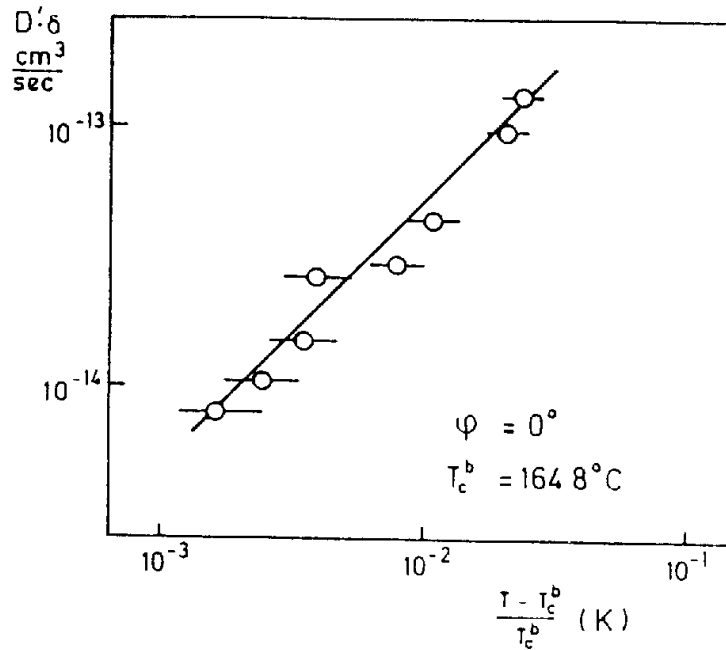


Fig. 11. The log-log dependence of  $D'\delta$  for an interphase Sn-Ge boundary with  $\phi = 0^\circ$  above  $T_c^b$  on the  $|T - T_c^b|$ . The critical index for  $D'\delta$  is  $1.0 \pm 0.1$ .<sup>50</sup>

can be seen from the diagram, a straight line is a good approximation of the experimental results, the tangent of the slope angle being equal to  $1.0 \pm 0.1$ . Therefore, the considered ideas provide an explanation for the anomalous decrease of the GB diffusion coefficient at  $T \Rightarrow T_c^b + 0$  and predict the correct value of the corresponding critical index. However, all the considerations presented must be valid both above and below the GB phase transition point. So the anomalous growth of indium diffusion coefficient at  $T \Rightarrow T_c^b - 0$  (see Fig. 8) remains unclear. Apparently<sup>50</sup> the decomposition (12), based on Landau theory, ceases to be valid. This is connected with the fact that fluctuations are strongly developed in part of the critical region which is closer to the first-order phase transition (stronger than at temperatures above the critical point).<sup>67</sup> The dimensionality  $d = 3$  is known to be marginal for a critical point of the type presented in Fig. 4. This means that the additional fluctuation terms of the thermodynamical parameters diverge logarithmically in three-dimensional space, while for  $d = 2$  they diverge according to the power law. Figure 12 displays the data on indium diffusion coefficient for an interphase boundary with  $\phi = 3$  below  $T_c^b$ , plotted in log-log coordinates. It can be seen that a straight line would be a good approximation (tangent of the slope is  $1.5 \pm 0.2$ ), which corresponds to power divergence. So, measuring the diffusion parameters of GBs, we really do obtain information about the thin two-dimensional layer (the problem of diffusion thickness of GBs is non-trivial and still remains a subject of discussions<sup>68</sup>).

## 9. Premelting Transition on Grain Boundaries in Alloys

In Ref. 51, premelting transition was discovered on GBs in the quasi-binary system Fe(Si)-Zn. This work dealt with zinc penetration along the symmetrical

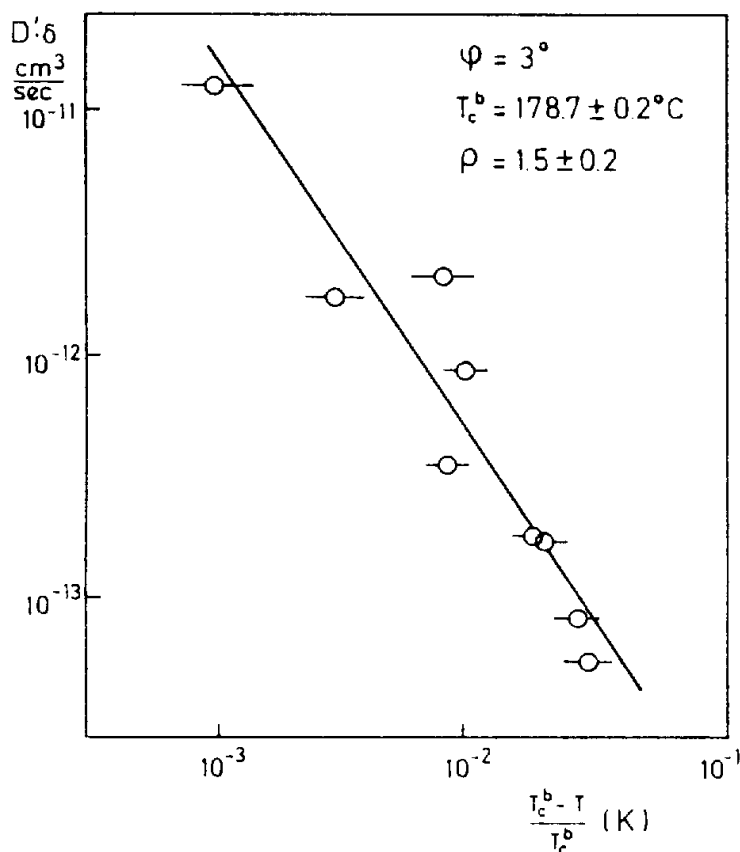


Fig. 12. The log-log dependence of  $D'\delta$  for an interphase Sn-Ge boundary with  $\phi = 3^\circ$  below  $T_c^b$  on the  $(T - T_c^b)$ . The critical index for  $D'\delta$  is  $1.5 \pm 0.2$ .<sup>50</sup>

tilt GB [100]  $43^\circ$  in Fe-5at%Si alloy. Zinc penetrated into the bicrystalline samples from a thick ( $\cong 100 \mu\text{m}$ ) surface layer. As has already been mentioned, complete wetting of GBs with zinc-base melt may be observed in this system. Actually, a thin ( $\cong 1 \mu\text{m}$ ) zinc-enriched layer was observed along the GBs in the whole of the studied temperature range (650 to  $975^\circ\text{C}$ ). Fisher's curves of zinc penetration along GBs, measured below the wetting interlayer, had knees at certain concentration  $c_{\text{bt}}$  (see Fig. 13 which presents a few such dependences). The  $c_{\text{bt}}$  value was shown to be independent of the annealing time. Consequently, this concentration is an equilibrium characteristic of a GB.

The temperature dependence of  $c_{\text{bt}}$  is displayed in Fig. 14. In this figure, the line of solubility limit of zinc in the Fe-5at%Si alloy and that of zinc in pure iron are displayed. Maximum solubility is observed at the peritectic temperature. The  $c_{\text{bt}}(T)$  line has a rather complicated form. Above the Curie point, the lower the  $c_{\text{bt}}$  concentration value, the greater is the bulk solubility limit  $c_0$ . In the vicinity of the Curie point this correlation is distorted: the line has a protuberance facing the lower zinc concentrations.

The hypothesis that at concentration  $c_{\text{bt}}$  a GB undergoes premelting transition (see Fig. 5) can serve as a basis for understanding the nature of knees on Fisher's dependences (Fig. 13) and explain the peculiarities of the GB phase diagram presented in Fig. 14. Actually, such a transition causes abrupt changes in both the

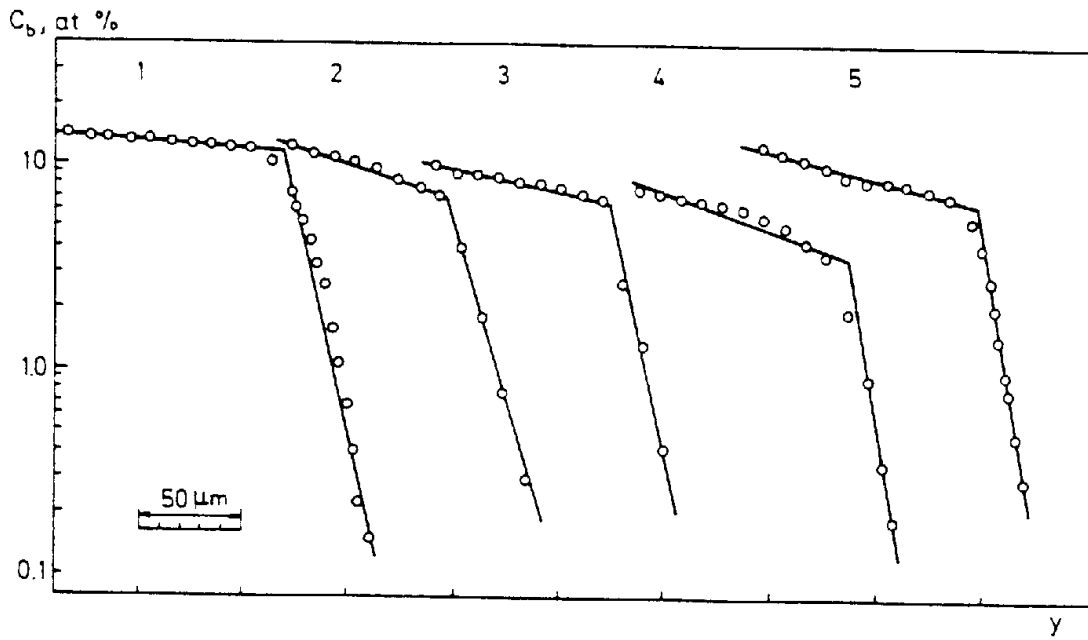


Fig. 13. The dependences of zinc concentration on boundaries  $c_b$  on depth  $y$  for different temperatures. At concentration  $c_{bt}$ , the value of product of diffusion coefficient and boundary width  $D\delta$  is changed abruptly. The product is measured by the slope of  $c_b(y)$  dependences. The  $c_{bt}$  concentration is changed with temperature. 1) 975°C, 1.75 h; 2) 857°C, 7.5 h; 3) 809°C, 21 h; 4) 790°C, 63 h; 5) 745°C, 102 h.

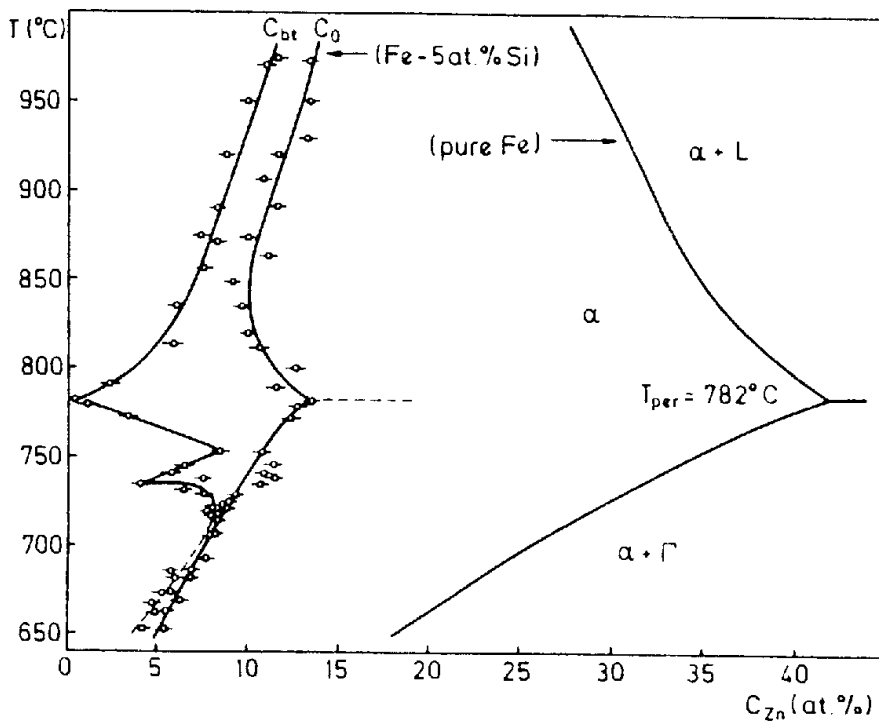


Fig. 14. The thermal dependences of  $c_{bt}$  and  $c_0$ . The zinc concentration is plotted on the x-axis. The line of solubility limit of zinc in pure iron is also displayed (solidus and solvus).  $\Gamma$  is an intermetallic compound and  $L$  is the liquid.

diffusion coefficient  $D'$  and the thickness of the layer of accelerated diffusion  $\delta$ . The ratio of the thickness of premelted layer formed on a GB, and the thickness of the GB itself, can be roughly estimated assuming the diffusion coefficients on the GB and in the quasi-liquid layer to be equal. This yields a value of  $10^2$  for the said ratio.

It is known that all the miscellany of wetting phenomena may be obtained from an analysis of the wetting layer free energy  $\Omega_s$ :

$$\Omega_s = 2\sigma_{ct} + l\Delta g + V(l) . \quad (13)$$

Here,  $\sigma_{ct}$  is the surface tension of the “crystal-wetting phase” interface,  $l$  is the wetting layer thickness,  $\Delta g$  is the excess free energy of the wetting phase. The latter term describes the interaction of the “crystal-wetting phase” interfaces. The situation that the wetting layer thickness goes into infinity ( $l \Rightarrow \infty$ ) when the line of phase co-existence is approached ( $\Delta g \Rightarrow 0$ ) is called complete wetting. Because the equilibrium thickness of the wetting layer is determined by minimization of (12) with regard to  $l$ , complete wetting can be observed only in the case when the two following conditions are satisfied:

$$\text{I: } 2\sigma_{ct} < \sigma_{gb} ,$$

where  $\sigma_{gb}$  the GB surface tension;

$$\text{II: } V(l) \text{ must have global minimum for } l = \infty .$$

In other words, the interfaces “crystal-wetting phase” must repel one another. We assume that  $V$  depends on  $l$  by a power law:

$$V(l) = W/l^n . \quad (14)$$

When  $c_b$  equals to the bulk solubility limit  $c_0$  (solvus or solidus) we have  $\Delta g = 0$ . For small deviations from  $c_0$  we shall expand  $\Delta g$  into a series in terms of  $c_0 - c_b$ . Truncation at the first term of this expansion yields

$$g = b(c_0 - c_b) . \quad (15)$$

The  $\Omega_s(l)$  function determined by the use of Eqs. (13), (14) and (15) has a minimum at  $l_0 = (b(c_0 - c_b)/nW)^{-1/(n+1)}$ .

$$\Omega(l_0) = \Omega_0 = 2\sigma_{ct} + (nW)^{1/(n+1)}(b(c_0 - c_b))^{n/(n+1)}(1 + n^{-1}) .$$

When the condition  $\Omega_0 = \sigma_{gb}$  is satisfied, premelting transition occurs: the GB is replaced by a layer of a phase enriched in zinc. From this condition we obtain

$$c_{bt} = c_0 - \frac{(\sigma_{gb} - 2\sigma_{cf})^{(n+1)/n}}{b(Wn)^{1/n}(1+n^{-1})^{(n+1)/n}}. \quad (16)$$

Equation (16) connects the bulk solubility limit with the concentration at which premelting transition occurs at the boundary. But the surface tensions  $\sigma_{gb}$  and  $\sigma_{cf}$  also depend on concentration, so it is not so easy to compare (16) with the experimental data. Luckily, in the system Fe-Zn the solubility limit line (solvus) is near to the metastable curve of solid solution decomposition (cf. Fig. 14). This means that the  $\sigma_{cf}$  value falls dramatically when the peritectics transformation point is approached. This, according to formula (16), must lead to a decrease in  $c_{bt}$ , which is actually observed in the experiment.<sup>49</sup>

Adding extra terms (corresponding to attraction of “crystal-melt” interfaces) may lead to the situation that this function ceases to have global minimum for  $l \Rightarrow \infty$ . Here, a transition from complete to incomplete wetting may occur, or the concentration range of premelted state stability may decrease. Such a term appears to be due to the transition of the Fe-Si alloy bulk into a ferromagnetic state. Remember that when a magnet is cut in two the parts attract each other. Accurate calculations<sup>69</sup> show that the “magnetic” part of the  $V(l)$  function is comparable with the “non-magnetic” part. Actually, at temperatures as low as 720°C (which is 20° lower than the Curie point in Fe-5at%Si alloy), the  $c_{bt}(T)$  line practically merges with the line of bulk solubility limit of zinc in the alloy (Fig. 14).

What about the protuberance directed towards lower concentrations on the  $c_{bt}(T)$  line near the Curie point? Such things are often observed at the intersection of a line of second-order phase transition with a line of first-order phase transition.<sup>70</sup> This can be illustrated within the framework of a simple thermodynamical theory.<sup>54</sup>

Now we see that the hypothesis of premelting transition can explain the behaviour of the  $c_{bt}(T)$  line near the peritectic temperature and below the Curie point. If function  $V(l)$ , which describes the interaction of “crystal-wetting phase” interfaces corresponds to a power law (14), then the premelting transition has to be accompanied by complete wetting of GB with the melt. It should be stressed that the inverse statement is wrong. For example (see above), the analysis of GB melting in pure metals shows that, though the wetting of a GB by the melt at the melting point is complete, at lower temperatures the parameter of long-range order in the GB plane has a non-zero value. Such a correlation between premelting and complete wetting can be used for verification of the premelting hypothesis. Imagine that, changing some thermodynamical parameters (pressure, impurity concentration), we have managed to transfer from complete to incomplete wetting of GB by the melt. If the region of accelerated GB diffusion

vanishes simultaneously with wetting (see Fig. 13), it will confirm that the region of rapid GB diffusion is connected with premelting transition. This idea was realized in Refs. 54 and 71.

The work in Ref. 71 is devoted to studies of the influence of high hydrostatic pressure on zinc penetration along the symmetrical tilt GB  $43^\circ$  [100] in Fe-6at%Si alloy at the annealing temperature  $905^\circ\text{C}$ . At a pressure of about 0.5 GPa, transition from complete to incomplete wetting of GB with zinc-based melt was observed. This transition was manifested in that the angle  $\theta$  at the tip of the GB groove was changed from zero (at pressure  $P < P_w \cong 0.5$  GPa) to nonzero values, increasing with  $P$  ( $P > P_w$ ). Such a transition is explained by the surface tensions of GBs,  $\sigma_{gb}$ , and of interphase boundaries,  $\sigma_{cf}$ , change with pressure in different ways. Simultaneously with the disappearance of complete wetting, the region of accelerated GB diffusion also vanishes from Fisher's dependences (Fig. 15). This confirms the hypothesis that the gentle regions on Fisher's dependences are connected with premelting transition.

The work in Ref. 52 was devoted to studies of zinc penetration along the symmetrical tilt GB  $38^\circ$ [100] in Fe-12at%Si alloy. An alloy with this silicon percentage undergoes atomic ordering: disorder bcc lattice ( $A_2$  structure) is transformed into an ordered one ( $B_2$  structure) at approximately  $770^\circ\text{C}$ . With a decrease of annealing temperature, transition from complete to incomplete wetting of GB by zinc-based melt was observed at  $T = 749 \pm 4^\circ\text{C}$ . Above this temperature, the  $\theta$  angle at the site of GB intersection with the surface was equal to zero (this corresponds to a thin wetting layer on the GB), while below this temperature  $\theta$  was approximately equal to  $\pi$ . It should be noted that  $T_w$ , the

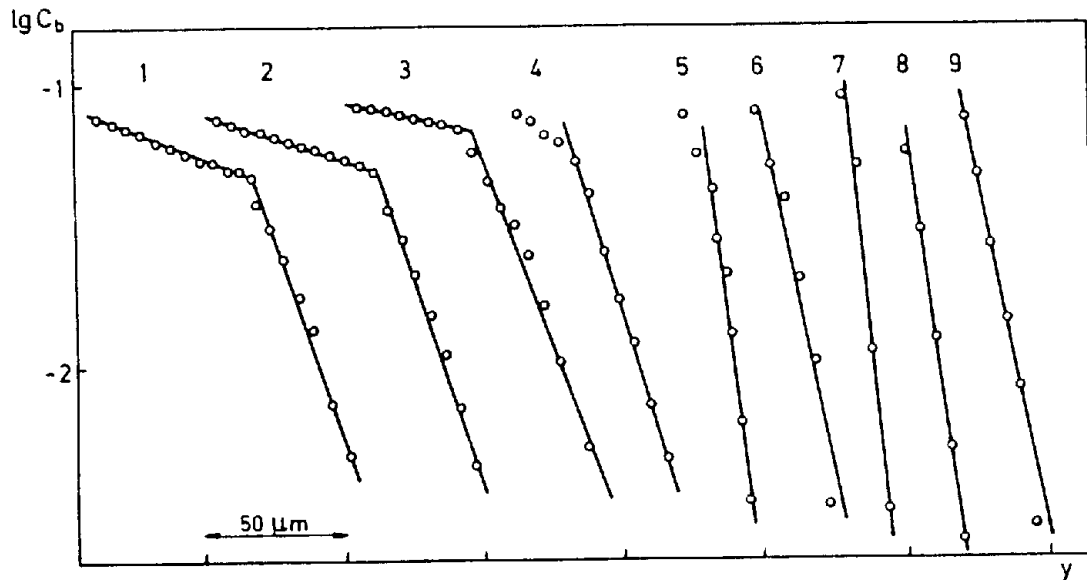


Fig. 15. Dependences of zinc concentration on grain boundaries  $c_b$  vs. depth  $y$  after annealing at temperature  $905^\circ$  for various pressure values in Fe-6 at.% Si bicrystals: 1 — 0.004 GPa; 2 — 0.05 GPa; 3 — 0.14 GPa; 4 — 0.35 GPa; 5 — 0.58 GPa; 6 — 0.74 GPa; 7 — 0.89 GPa; 8 — 1.17 GPa; 9 — 1.4 GPa.



temperature of wetting transition, is slightly lower than  $T_{\text{ord}}$ , the temperature of bulk atomic ordering. This can be easily understood. Atomic ordering can be considered as formation of additional bonds between atoms of different types which leads to decrease of total free energy of the alloy. Wetting layer destroys all such bonds while at the GB they are partially preserved. Therefore, the positive contribution of bulk ordering to  $2\sigma_{\text{cf}}$  greater than that to  $\sigma_{\text{gb}}$ . The maximum growth of the order parameter in the ordered phase takes place in the range of several tens of degrees below the phase transition point.<sup>72</sup> Therefore, the most abrupt change of surface tension occurs also in this interval. The difference  $T_{\text{ord}} - T_{\text{w}}$  is of this order of magnitude. It should be noted that the difference between  $T_{\text{c}}^{\text{h}}$ , the temperature of GB prewetting transition in tin, and  $T_{\text{c}}$ , the temperature of the bulk transition, is also between 17 and 25°C.

In this work, as well as in Ref. 71, the gentle region of Fisher's dependences was found to vanish simultaneously with wetting (see Fig. 16). This confirms once more that the gentle regions on Fisher's dependences are connected with premelting transition. Some other interesting phenomena were also discovered in

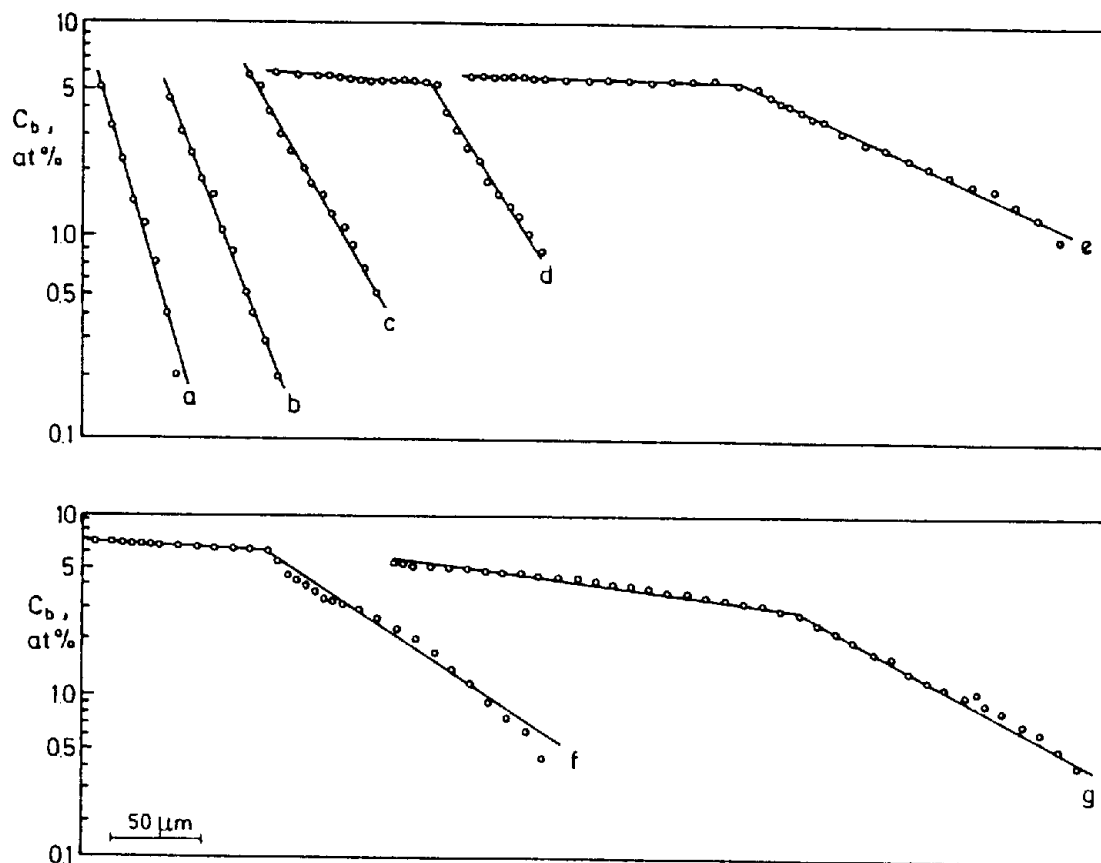


Fig. 16. The dependences of grain boundary zinc concentration  $c_b$  vs. the depth  $\gamma$  (the curves of zinc diffusional penetration along the grain boundaries). The concentration  $C_{\text{bt}}$  corresponds to the knees on the dependences  $C_b(\gamma)$ : a — 724°C, 241 h; b — 734°C, 184 h; c — 754°C, 110.5 h; d — 764°C, 65 h; e — 774°C, 50 h; f — 784°C, 50 h; g — 804°C, 30 h; h — 810°C, 18 h; i — 830°C, 10 h; j — 834°C, 14 h; k — 844°C, 10.2 h; l — 874°C, 6.5 h; m — 934°C, 5 h; n — 994°C, 4.5 h.

the discussed work. Analysis of the Fisher's dependences presented in Fig. 16 shows that the sharp knee connected with premelting transition vanishes at temperatures above  $T_{\text{crit}} = 801 \pm 2^\circ\text{C}$ . The dependences themselves are somehow bent in this region. Here, "traces" of the gentle region still remain, which are revealed in the large (as compared with previously known values) GB diffusion coefficient. Such unusual behaviour of zinc penetration along GB can be understood on the assumption that there exists a tricritical point of GB premelting (at temperature  $T_{\text{crit}}$ ), which separates the first-order premelting transition ( $T < T_{\text{crit}}$ ) from the second-order premelting transition ( $T > T_{\text{crit}}$ ). The schematical diagram in Fig. 17 illustrates the difference between the first-order and second-order premelting transitions. In the first case, the long-range order parameter falls abruptly during continuous increase of zinc concentration in a GB, while in the second case the said parameter changes also continuously. At temperature  $T_{\text{cont}}$ , the line of second-order phase transitions contacts with the line of zinc solubility limit (solvus). At temperatures  $T > T_{\text{cont}}$  the situation is similar to the case of GB in pure metals: GB is wet by the melt completely, but the long-range order parameter approaches zero in the GB plane no earlier than the solvus concentration is reached (premelting is absent). The GB phase diagrams summarizing all the above considerations are presented in Figs. 18 and 19. In Fig. 18 experimental points are shown, while in Fig. 19 second-order GB premelting transitions are plotted as dotted lines. Unfortunately, we cannot determine from our measurements the exact concentration at which second-order transition occurs, so Fig. 19 has schematic sense only. The temperature dependence of GB diffusion coefficient determined by the slope of Fisher's dependences also turned out quite unusual (see Fig. 20). In the temperature range between  $T_{\text{crit}}$  and  $T_{\text{cont}}$ , an interesting effect is observed: GB diffusion coefficient decreases with temperature growth. This may be connected with the decrease of the concentration region of quasi-liquid interface existence, which affects the

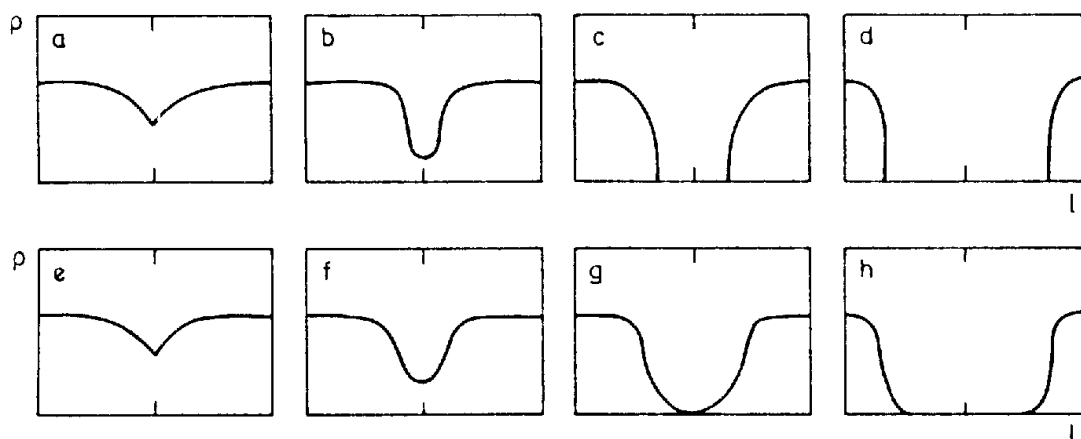


Fig. 17. The schematic dependences of long-range order parameter  $\rho$  in the atomic layers parallel to the grain boundary upon the distance from the grain boundary  $l$ . a–d — first order premelting transition, e–h — second order premelting transition. At the first order transition  $\rho$  values near the boundary jump from non-zero value to zero when increasing the temperature. At the second-order transition the order parameter changes smoothly.

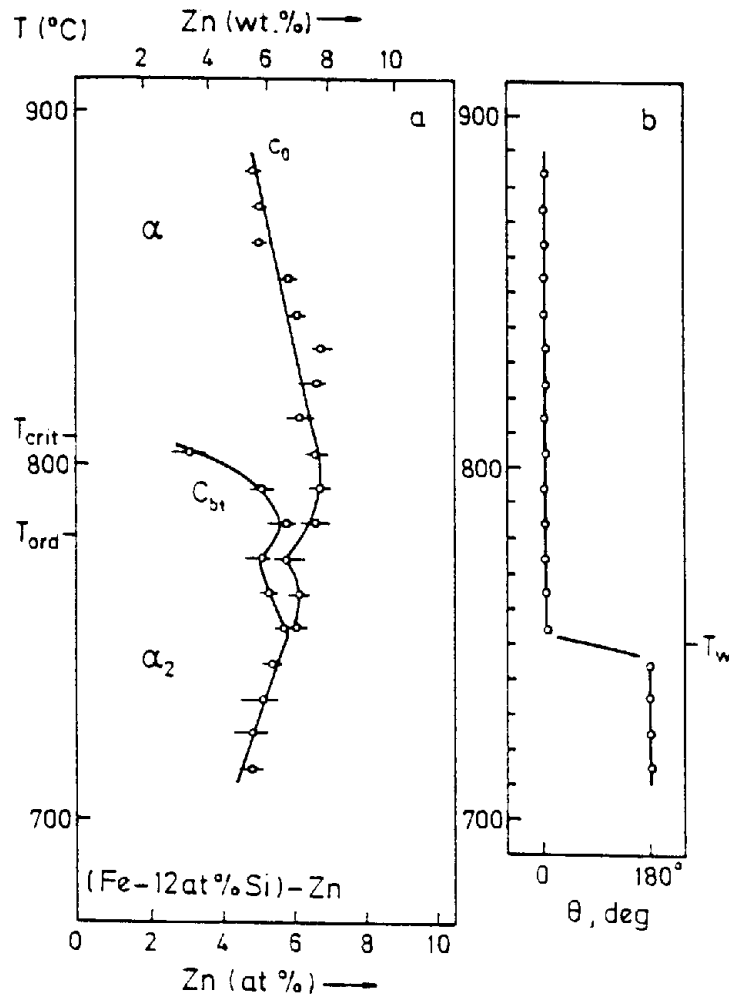


Fig. 18. a) The temperature dependences of Zn concentrations  $c_{bt}$  and  $c_0$  for Fe-12 at.% Si alloy.  $T_{ord}$  — temperature of the bulk ordering  $A_2-B_2$ ;  $T_{crit}$  — the critical point on the line  $c_{bt}(T)$  of grain boundary premelting transition. b) Temperature dependence of the angle  $\theta$  in the site of the grain boundary intersection with the surface.  $T_w$  — temperature of grain boundary wetting transition.

effective slope of Fisher's dependences. The anomaly near  $T_{ord}$  may be connected with the critical behaviour of the thermodynamical factor for GB diffusion coefficient in the vicinity of the bulk ordering temperature.

The results of Refs. 51, 52 show that ordering (atomic, spin) suppresses wetting transition, as well as the associated premelting transition. Actually, in the work,<sup>73</sup> which dealt with zinc penetration along the tilt GB  $38^\circ$  [100] in Fe-10at%Si alloy, complete wetting and associated premelting were surely observed down to the lowest studied temperature, 700°C. In the alloy Fe-10at%Si, only spin ordering is present at about 700°C. Again as in Ref. 52, a tricritical point of phase transition at temperature  $T_{crit} \approx 810^\circ\text{C}$  was found in Ref. 73 "Traces" of the gentle region on Fisher's dependences were observed in Ref. 73 up to the higher limit of the studied temperature range. This means that either  $T_{cont}$  for Fe-10at%Si alloy is above the studied temperature range, or the premelting transition line ends on the line corresponding to pure (without zinc) Fe-10at%Si alloy.

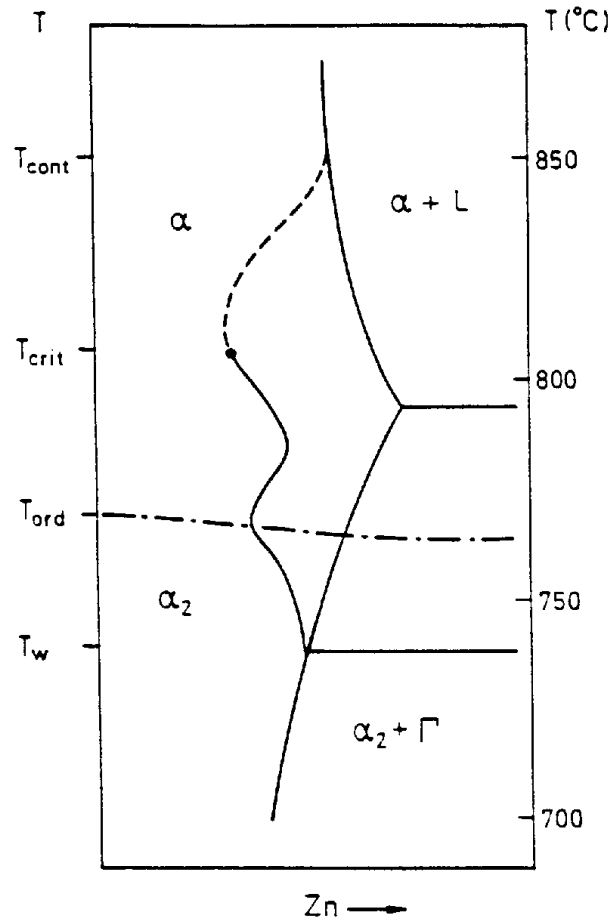


Fig. 19. The schematic grain boundary phase diagram ( $c_{bt}$  and  $c_0$  dependences for Fe-12 at.% Si alloy), where the line of second-order grain boundary premelting transition is shown.

Therefore, the set of data of zinc penetration along the GBs in Fe-Si alloys obtained in works<sup>51,52,71,73</sup> indicates that GB premelting transition occurs in the system Fe-Si-Zn.

## 10. Some Ideas Regarding Directions of Further Research

1. More detailed investigation of GB wetting transition and complete wetting by the melt. In spite of the large amount of existing data, many important questions still remain unanswered: what is the dependence of the phase transition point upon the GB type; what is the order of the wetting transition, and what is determined by it, etc.? For example, to determine the order of the wetting transition, it is necessary to measure the temperature dependence of the angle  $\theta$  at the tip of the GB groove accurately in a narrow temperature range below the wetting transition temperature  $T_w$ . This dependence is continuous for both first- and second-order phase transitions. They can be distinguished only by the power of the law correlating  $T$  with  $|T - T_w|$ .<sup>74</sup> As far as we know, such studies have not yet been carried out.
2. Search for new systems in which the prewetting and premelting phenomena

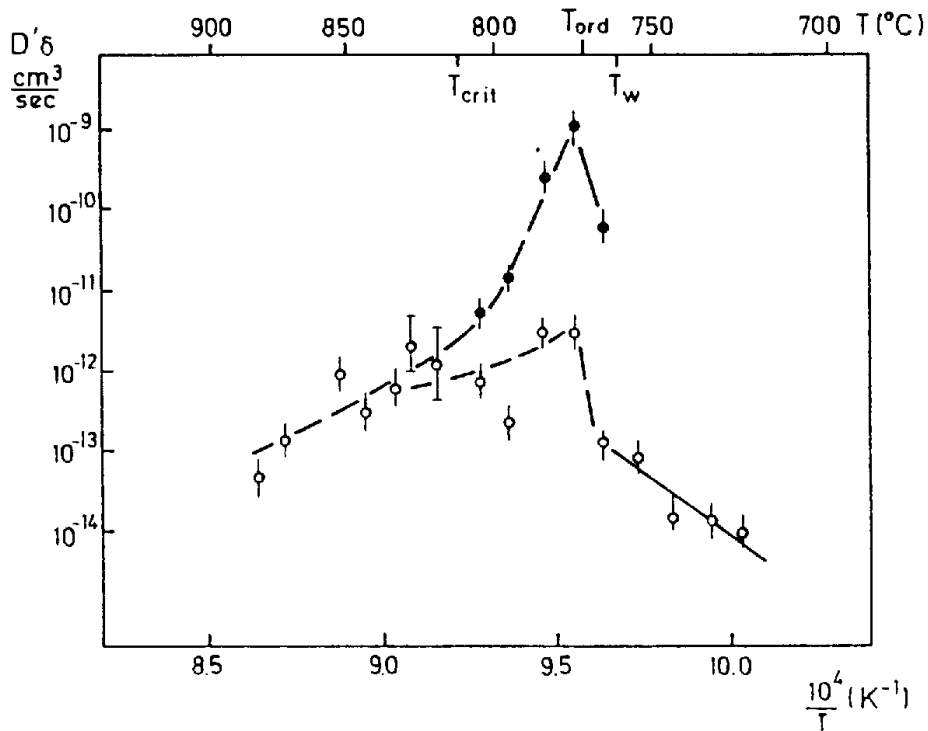


Fig. 20. The temperature dependence of the grain boundary diffusion permeability  $D'\delta$  for Zn in Fe-12 at.% Si alloy. Black points correspond to concentrations in range from  $c_0$  to  $c_{bl}$ .

are present, along with a search for new methods of uncovering these effects. The systems Sn-In and Fe-Si-Zn are so far unique to exhibiting prewetting and premelting transitions. Besides, while quite complete, the studies<sup>49-52,69,73</sup> are indirect. For example, some phases from the stable phase diagram are known not to be formed in the interdiffusion zone. Besides, the phases, which do form under the said conditions can have regions of stability, shifted with respect to the equilibrium ones.<sup>58</sup> So, the problem of direct observation of GB prewetting and premelting transitions and that of search for alternative indirect methods of investigation of these transitions remain. Here a work<sup>75</sup> should be mentioned, where the phenomenon of complete wetting of antiphase domain walls by disordered phase in  $\text{CoPt}_3$  alloy was studied. In this work the temperature anomalies of electroconductivity (or, more precisely, its derivative) served as a tool for investigating the transitions.

3. Search for new types of GB phase transitions, as well as plotting of complete GB phase diagrams. Besides the discussed ones, some other GB phase transitions can be imagined. For example, research on phase transition "two-dimensional paramagnet — two-dimensional ferromagnet" which occurs during adsorption of magnetic impurity on a GB in a paramagnetic matrix seems to be useful. Here various structures can be formed. For example, since the sign of exchange interaction is strongly dependent on the interatomic distance, the following pattern can be imagined: antiferromagnetic chains along the SGBD lines, separated by the ferromagnetic strips.

Grain boundary phase diagrams were first obtained in the works of Refs. 51, 52, 73. The lines of these diagrams consist of GB premelting transition points. However, as we have already seen, there exist also other GB phase transitions, in both alloys and pure metals. So it is interesting to investigate the mutual influence of the various phase transitions. By such data, complete GB phase diagrams can be plotted, in analogy to bulk or surface phase diagrams. Such diagrams could find important practical applications.

4. Development of a theory of wetting phenomena on GBs. Such a theory must predict systems where wetting, prewetting and premelting transitions can be observed, and the parameters of such transitions. Since an object as "simple" as the GB structure of pure metals at zero temperature can be studied theoretically only by computer simulation, it is clear that numerical calculations are the basic tool for such research. Only in this way can a satisfactory agreement with the experimental data be obtained.

### Acknowledgments

One of us (B. B. S.) wishes to thank Alexander von Humboldt Foundation for the support of his work in MPI für Metallforschung (Stuttgart).

### References

1. Proceedings of the International Congress on *Intergranular and Interphase Boundaries in Materials*, *J. Physique* **51**, Suppl. 1.
2. W. Bollman, *Crystal Defects and Crystalline Interfaces* (Springer, 1970).
3. R. W. Balluffi, in *Interfacial Segregation*, ed. W. C. Johnson and J. M. Blakely (ASM, Metals Park, 1977).
4. A. P. Sutton and R. W. Balluffi, *Acta Metall.* **35**, 2177 (1987).
5. A. P. Sutton and V. Vitek, *Phil. Trans. Roy. Soc. London* **A309**, 1 (1977).
6. G.-J. Wang and V. Vitek, *Acta Metall.* **34**, 951 (1986).
7. E. M. Fridman, Ch. V. Kopetsky and L. S. Shvindlerman, *Fiz. Tverdogo Tela*, **16**, 1771 (1973) (in Russian).
8. M. E. Glicksman and C. L. Vold, in *Solidification* (ASM, Metals Park, 1971).
9. C. Rottman, *Scripta Metall.* **19**, 43 (1985).
10. T. E. Hsieh and R. W. Balluffi, *Acta Metall.* **37**, 1637 (1989).
11. G. Ciccotti, M. Guillope and V. Pontikis, *Phys. Rev.* **B27**, 5576 (1983).
12. T. Nguen, P. S. Ho, T. Kwok, C. Nitta, and S. Yip, *Scripta Metall.* **19**, 993 (1985).
13. T. Nguen, P. S. Ho, T. Kwok, C. Nitta, and S. Yip, *Phys. Rev. Lett.* **57**, 1919 (1986).
14. J. Q. Broughton and G. H. Gilmer, *Phys. Rev. Lett.* **56**, 2692 (1986).
15. S. M. Foiles, M. I. Baskes and M. S. Daw, *Phys. Rev.* **B33**, 7983 (1986).
16. J. F. Lutsko and D. Wolf, *Scripta Metall.* **22**, 1923 (1988).
17. E. S. Bokstein, L. M. Klinger and L. S. Shvindlerman, *Jurn. Fiz. Chim.* **48**, 1527 (1974) (in Russian).
18. W. A. Curtin, *Phys. Rev. Lett.* **59**, 1228 (1987).
19. R. Kikuchi and J. W. Cahn, *Phys. Rev.* **B21**, 1893 (1980).
20. R. Kikuchi and J. W. Cahn, *Phys. Rev.* **B36**, 418 (1987).
21. B. Derrida and M. Schick, *J. Phys.* **A19**, 1439 (1986).

22. J. W. M. Frenken, P. M. J. Maree and J. F. van der Veen, *Phys. Rev.* **B34**, 7506 (1986).
23. B. Pluis, A. W. Denier van der Gon, J. F. van der Veen, and A. J. Riemersma, to appear in *Surface Sci.*
24. T. Schober and R. W. Balluffi, *Phil. Mag.* **20**, 511 (1969).
25. K. F. Sickafus and S. L. Sass, *Acta Metall.* **35**, 69 (1987).
26. C.-H. Lin and S. L. Sass, *Scripta Metall.* **22**, 735 (1988).
27. C.-H. Lin and S. L. Sass, *Scripta Metall.* **22**, 1569 (1988).
28. Ch. V. Kopetsky, A. N. Orlov and L. K. Fionova, *Grain Boundaries in Pure Materials* (Nauka, Moscow, 1987), p. 160 (in Russian).
29. T. E. Hsieh and R. W. Balluffi, *Acta Metall.* **37**, 2133 (1989).
30. T. G. Ference and R. W. Balluffi, *Scripta Metall.* **22**, 1929 (1988).
31. T. Watanabe, S.-I. Kimura and S. Karasima, *Phil. Mag.* **A49**, 845 (1984).
32. E. L. Maksimova, L. S. Shvindlerman and B. B. Straumal, *Acta Metall.* **36**, 1573 (1988).
33. E. L. Maksimova, E. I. Rabkin, L. S. Shvindlerman, and B. B. Straumal, *Acta Metall.* **37**, 1995 (1989).
34. J. W. Cahn, in *Interfacial Segregation*, ed. W. C. Johnson and J. M. Blakely (ASM, Metals Park, 1977).
35. H. Gleiter, *Scripta Metall.* **11**, 305 (1977).
36. D. Farkas and H. Jang, *Scripta Metall.* **22**, 1431 (1988).
37. V. G. Sursaeva, Ch. V. Kopetsky and L. S. Shvindlerman, *Scripta Metall.* **12**, 953 (1978).
38. A. Passerone, N. Eustathopoulos and P. Desré, *J. Less Common Metals.* **52**, 37 (1977).
39. A. Passerone and R. Sangiorgi, *Acta Metall.* **33**, 771 (1985).
40. K. K. Ikeuye and C. S. Smith, *Trans. AIME* **185**, 762 (1949).
41. N. Eustathopoulos, L. Coudurier, J. C. Joud, and P. Desre, *J. Crystal Growth* **33**, 105 (1976).
42. J. H. Rogerson and J. C. Borland, *Trans. AIME* **227**, 2 (1963).
43. A. Passerone, R. Sangiorgi, and N. Eustathopoulos, *Scripta Metall.* **16**, 547 (1982).
44. J. W. Cahn, *J. Chem. Phys.* **66**, 3667 (1977).
45. C. Hammond, *Phys. Technol.* **14**, 263 (1983).
46. R. Z. Valiev, V. Yu. Gertsman and O. A. Kaibyshev, *Phys. Stat. Sol.* **97A**, 11 (1986).
47. J. W. Cahn, *J. Physique* **43**, C199 (1982).
48. P. Guiraldeng and P. Lacombe, *Acta Metall.* **13**, 51 (1965).
49. E. I. Rabkin, L. S. Shvindlerman and B. B. Straumal, *J. Less Common Metals.* **158**, 23 (1990).
50. E. I. Rabkin, L. S. Shvindlerman and B. B. Straumal, *J. Less Common Metals* **159**, 43 (1990).
51. E. I. Rabkin, V. N. Semenov, L. S. Shvindlerman, and B. B. Straumal, *Acta Metall. Mater.* **39**, 627 (1991).
52. O. I. Noskovich, E. I. Rabkin, B. B. Straumal, and V. N. Semenov, *Scripta Metall.* **25**, 1441 (1991).
53. O. Kubaschewski, *Iron-binary Phase Diagrams* (Springer-Verlag, 1982), p. 169.
54. T. Nishizawa, M. Hasebe, and M. Ko, *Acta Metall.* **27**, 817 (1979).
55. J. C. Fisher, *J. Appl. Phys.* **22**, 74 (1951).
56. S. Havlin and D. Ben-Avraham, *Adv. Phys.* **36**, 695 (1987).
57. T. Suzuoka, *Trans. Jap. Inst. Met.* **2**, 25 (1961).
58. K. P. Gurov, B. A. Kartashkin and Yu. E. Ugaste, *Interdiffusion in Many-Phase Metallic Systems* (Nauka, Moscow, 1981), p. 87 (in Russian).

59. L. A. Bolshov and M. S. Veshunov, *Sov. Phys. JETP* **95**, 2039 (1989).
60. H. E. Stanley, *Introduction to Phase Transitions and critical Phenomena* (Clarendon Press, Oxford, 1971), p. 268.
61. Yu. S. Vedula, A. T. Loburets and A. G. Naumovets, *Sov. Phys. JETP* **77**, 773 (1979).
62. I. F. Luksutov and V. L. Pokrovsky, *Sov. Phys. JETP Lett.* **33**, 343 (1981).
63. B. C. Giessen, *Advances in X-Ray Analysis, vol. 12* (Plenum, New York, 1969), p. 23.
64. B. B. Straumal, L. M. Klinger and L. S. Shvindlerman, *Acta Metall.* **32**, 1355 (1984).
65. P. G. De Gennes, *Rev. Mod. Phys.* **57**, 827 (1985).
66. R. Pandit, M. Schick and M. Wortis, *Phys. Rev.* **B26**, 5112 (1982).
67. M. A. Krivoglaz, *The Theory of X-Rays and Thermal Neutrons Scattering by Real Crystals* (Nauka, Moscow, 1967), p. 34 (in Russian).
68. Yu. M. Mishin and I. M. Razumovsky, *Poverhnost* **1**, 82 (1982) (in Russian).
69. E. I. Rabkin, L. S. Shvindlerman and B. B. Straumal, *J. Physique* **51**, C599 (1990).
70. *Alloy Phase Diagrams*, edited by L. H. Bennett, T. B. Massalski and B. C. Giessen (North-Holland, 1983).
71. L. S. Shvindlerman, W. Lojkowski, E. I. Rabkin, and B. B. Straumal, *J. Physique* **51**, C629 (1990).
72. H. H. Potter, *Proc. Roy. Soc. Lond.* **146**, 362 (1934).
73. B. B. Straumal, O. I. Noskovich, V. N. Semenov, L. S. Shvindlerman, W. Gust, and B. Predel, *Acta Metall. Mater.*, in press.
74. S. Dietrich, in *Phase Transitions and Critical Phenomena*, ed. C. Domb and J. Lebowitz, vol. 12 (Academic Press, 1988).
75. Ch. Leroux, A. Loiseau, M. C. Cadeville, and F. Ducastelle, *Europhys. Lett.* **12**, 155 (1990).
76. E. L. Maksimova, L. S. Shvindlerman and B. B. Straumal, *Acta Metall.* **37**, 2855 (1989).